



Engineering and
Physical Sciences
Research Council



An Electrochemical Biosensor for Sensitive in-situ Detection of Methyl- isoborneol (MIB) in Water.

Research completed by: Joshua Pearce

Academic Supervisor: Dr Wei Zhang

Date Submitted: 01/01/25

Submitted to Swansea University in fulfillment of the requirements for the Degree of
Masters of Research in Materials Engineering

Abstract

2-Methylisoborneol (MIB) is a naturally occurring, odour producing compound which generates mass complaints due to its occurrence in drinking water. Removal and detection techniques are currently limited in the field due to the low detection level to the human nose being as low as 25ng/L. Current detection techniques consist of Gas Chromatography – Mass Spectrometry (GC/MS) which can struggle at detection levels such as this. This project will explore the potential of a sensing method which has both isolated selectivity to the target compound and has the ability for in-situ detection using an electrochemical biosensor, capable through the use of molecularly imprinted polymer (MIP) technology. The Brunner-Emmet-Teller (BET) nitrogen adsorption analysis, Raman spectroscopy and Scanning Electron Microscopy (SEM) were all used to characterize the sensor, while Cyclic voltammetry (CV) and Electrochemical impedance spectroscopy (EIS) were both used to analyse the electrochemical behaviour of the sensor. Ideal polymer conditions were found to be 10mL using a drop casting method, followed by a 48hour period in an oven at 40°C, with a sensor using a graphene, diacetone alcohol (DAA) and polydopamine (PDA) recipe was used on a Kapton polyimide tape. A template removal and reintroduction period of 25 minutes was found to be optimal, with the removal solution being a 1% ethanol mix with deionised water. Using the calibration curve from EIS testing, an LOD value of 1.45ng/L and LOQ value of 4.39ng/L were calculated.

Declarations and Statements

This work has not previously been accepted in substance for any degree and is not being concurrently submitted in candidature for any degree.

Signed: J.Pearce

Date: 01/01/25

This thesis is the result of my own investigations, except where otherwise stated. Other sources are acknowledged by footnotes giving explicit references. A bibliography is appended.

Signed: J.Pearce

Date: 01/01/25

I hereby give consent for my thesis, if accepted, to be available for photocopying and for interlibrary loan, and for the title and summary to be made available to outside organizations.

Signed: J.Pearce

Date: 01/01/25

The University's ethical procedures have been followed and, where appropriate, ethical approval has been granted.

Signed: J.Pearce

Date: 01/01/25

Table of Contents

Abstract	2
Declarations and Statements	3
Table of Contents	4
List of Tables	7
List of Figures	Error! Bookmark not defined.
Acknowledgements	11
Chapter 1 Introduction	12
1.1 Importance of Water Quality Monitoring.....	12
1.2 Challenges in Detecting 2-Methylisoborneol.....	14
1.3 Research Objectives	17
1.4 Environmental Impact and Technological Advancement.....	18
Chapter 2 Literature Review	20
2.1Chromatography-based methods for detection of MIB and geosmin	20
2.1.1 GC-MS	20
2.1.2 HPLC-MS.....	26
2.2 Colorimetric Methods for detection of MIB and geosmin	26
2.3 BMD from US-EPA.....	27
2.4 Sensors used for detection of MIB and geosmin.....	28
2.4.1 Quartz crystal microbalance (QCM) sensors	31
2.4.2 Electrochemical sensors	32
2.4.3 Electronic tongues and noses	34
2.5 Conclusions, challenges, and future developments.....	44
Chapter 3 Theoretical Background	48

3.1 Electrochemical Properties	48
3.1.1 Redox Reactions and Electrode Potentials	48
3.1.2 Types of Electrochemical Sensors	48
3.2 Analytical Techniques for Sensor Characterisation.....	49
3.2.1 Cyclic Voltammetry	49
3.2.2 Electrochemical Impedance Spectroscopy	50
3.3 Material Characterisation	51
3.3.1 Scanning Electron Microscopy (SEM).....	51
3.3.2 Raman Spectroscopy	52
3.3.3 BET nitrogen adsorption analysis	52
3.4 Principles of Molecular Imprinting Method.....	53
Chapter 4 Materials and Methodology.....	55
4.1 Chemicals and Reagents.....	55
4.2 Electrochemical Sensor Fabrication via Flexographic Printing	55
4.3 Preparation of the MIP sensors.....	56
4.3.1 Compound Selection for the Polymer	56
4.3.2 Polymerization Process and Conditions	56
4.3.3 Template Molecules Removal	57
4.4 Cyclic Voltammetry Testing	58
4.5 Electrochemical Impedance Spectroscopy	58
Chapter 5 Results and Discussion	60
5.1 Electrochemical MIP Sensor Preparation and Optimization.....	60
5.2 Template Molecules Removal	64
5.3 Reintroduction of the Target Molecules	67

5.4 MIP Sensor Characterization.....	69
5.5 Electrochemical Sensing Performance	74
5.6 Result Implication and Discussion	76
Chapter 6 Conclusion.....	78
Bibliography.....	80
Appendices: Materials and Methodology	90

List of Tables

Table 1: GC-MS along with different preconcentration techniques for detection of MIB and geosmin.....	21
Table 2: Determination of MIB and geosmin based on sensing methods.....	30
Table 3: Compound selection for MIPs with differing target molecules and their removal solutions	Error! Bookmark not defined.

List of Figures

Figure 1: Chemical structure of (a) MIB and (b) geosmin.....	14
Figure 2: Number of publications per year on geosmin and 2-MIB based on a literature search (Scopus) depicting the relevance of geosmin/ 2-MIB events over the years (1990- June 2020) [2]	15
Figure 3: (a) Schematic representation of the passive sample device for detection of MIB and geosmin. Reprinted with the permission of [35]; (b) Schematic illustration of the vacuum-assisted headspace solid-phase microextraction (VA-HS-SPME) assemble. Reprinted with the permission of [51].....	25
Figure 4: Components of a general electrochemical sensor. Reprinted with the permission of [62].....	32
Figure 5: (a) The TEM image of nanoparticle-embedded nanocarbon film (Pt-Nc). Reprinted with the permission of [64]; (b) The use of the Pt-Nc film for detection of geosmin. Reprinted with the permission of [64]; (c) The geosmin-imprinted polymer-based electrochemical sensor used for determining geosmin in water. Reprinted with the permission of [63]; (d) CV variations in regard of different geosmin concentrations ranging from 5 to 200 ng/L. Reprinted with the permission of [63].	33
Figure 6: Electrochemical impedance spectroscopy equipment used throughout testing	51
Figure 7: Scheme of Molecular Imprinting [109]	54
Figure 8: The copper strip surface (left) and gold electrode surface (right) through a microscope	56
Figure 9: The carbon electrode surface before (left) and after (right) MIP application.	57
Figure 10: Explosive (left) and top-down (right) view of an example carbon electrode, showing the MIP, epoxy, carbon and polyimide layers.	57
Figure 11: Overall (Left) and enlarged (Right) template removal technique with beaker, sensor, removal solution and stirrer.	58

Figure 12: EIS testing setup with multiple outputs, using the OCTOSTAT, showing the 2-electrode setup used throughout testing	60
Figure 13: Cyclic voltammetry results from a clean gold electrode	61
Figure 14: Cyclic voltammetry results from a clean copper strip	61
Figure 16: Cyclic voltammetry results from a carbon-based electrode following a 15-minute oven curing time.....	62
Figure 17: Cyclic voltammetry results from sensors post polymer application from 4 to 10 μ L, in 2 μ L increments.....	63
Figure 18: Cyclic voltammetry results from a sensor before and after the application of polymer.....	64
Figure 19: Nyquist plot results from a methanol and acetic acid mixture used as the washing solution for an initial test using NIP, 1-minute and 2-minute removal time.	64
Figure 20: Nyquist plot results from a 100% ethanol solution used as the washing solution with an MIP layer for an initial test to 40-minute removal time using 10-minute increments.....	65
Figure 21: Nyquist plot results from a 100% ethanol solution used as the washing solution with an NIP layer for a 10-minute to 40-minute removal time using 10-minute increments.....	65
Figure 22: Nyquist plot results from a 100% ethanol solution used as the washing solution with an MIP layer for an initial test (post polymer application) to 40-minute removal time using 10-minute increments.....	66
Figure 23: Nyquist plot results from a 100% ethanol solution used as the washing solution with an MIP for a 10-minute to 40-minute removal time using 10-minute increments.....	66
Figure 24: Bode plot from Electrochemical Impedance Spectroscopy of an NIP washed with 1% ethanol in an ultrasonic bath between 5 and 25 minutes, in 5 minutes intervals.	67

Figure 25: Nyquist plot from Electrochemical Impedance Spectroscopy of an NIP washed with 1% ethanol in an ultrasonic bath between 5 and 25 minutes, in 5 minutes intervals.	67
Figure 26: Bode plot from Electrochemical Impedance Spectroscopy of an MIP through stages of removal and reintroduction of the target molecule.....	68
Figure 27: Nyquist plot from Electrochemical Impedance Spectroscopy of an MIP through stages of removal and reintroduction of the target molecule.....	68
Figure 28: Bode plot from Electrochemical Impedance Spectroscopy of an MIP during reintroduction time optimization testing.....	69
Figure 29: Electron micrographs showing the surface morphologies of the interdigitated surface of a sensor following (a) non-imprinted polymer application, (b) imprinted polymer application, (c) post template removal of an imprinter sensor and (d) post reintroduction of the target molecule. Columns increase in magnification from left to right, with fields of view of 100, 20 and 5 μm	70
Figure 30: Raman spectroscopy data for the commercial graphene used in the fabrication of the sensor	71
Figure 31: Raman spectroscopy data for both a molecularly imprinted polymer covered sensor (blue) and pre molecularly imprinted polymer application (grey)....	72
Figure 32: BET nitrogen adsorption analysis data for an uncovered sensor.....	73
Figure 33: Randle circuit layout using both C and Q elements.	74
Figure 34: Calibration curve obtained for MIP using EIS data.....	75
Figure 35: FlexiProof Rolling press printer used for sensor production.....	90
Figure 36: Oven used for sensor optimisation	90
Figure 37: Finalisation of printing process on polyimide sheet.....	91

Acknowledgements

I would like to express my sincere gratitude to the following individuals for their invaluable contributions and support throughout this project:

- **Matthew Pagett:** Thank you for your guidance in all forms during this project, from teaching basic lab skills and understanding to explaining specialist lab techniques, your contributions to this project has been invaluable.
- **Lab Support Team:** Thank you to the whole lab support team for the technical expertise and commitment to ensuring the maintenance of the lab and equipment.
- **Prof. Chadly Tizaoui:** I am very grateful for allowing the use of certain lab resources and always being available for any insight that was needed.
- **Dr. Wei Zhang:** A special thank you for the guidance and expertise in both laboratory testing and specialist writing assistance throughout the project which have truly been irreplaceable.
- **The M2A and Welsh Water:** Thank you for the opportunity to carry out this research and allowing the opportunities to present the research. Without the continued support, it would not have been possible.

Chapter 1 Introduction

1.1 Importance of Water Quality Monitoring

Water quality maintenance and monitoring is a problem for society that dates back as far as 2880 B.C, with the beginning of the development towards understanding watershed management [1].

This is largely due to the size of the impact which water quality can have on life and industries around the globe, it is crucial for ensuring public health, environmental protection, and the sustainable use of water resources.

Water quality monitoring covers a wide range of issues, from taste and odour to chemical contamination. The pollution of surface water has become an issue that is growing worldwide as the understanding of its effect on both aquatic life and public health has been a larger research focal point. Pollution can come in the form of excess nutrients or toxic chemicals from storm water runoff, vadose zone leaching, groundwater discharges and oil spills [2].

Taste and odour perception of tap water is a critical issue to both water treatment industries and regular people as the alternative is usually a more expensive bottled water. This issue is predominantly caused by algal blooms within cyanobacteria, leading to the production of the two most common taste and odour compounds worldwide, being geosmin and 2-methylisoborneol (2-MIB) [3]. These compounds can be detected by humans at incredibly low concentrations, leading to the public to believe that the unpleasant taste or odour is due to some form of health risk in the water [4].

Access to clean and safe drinking water is crucial for maintaining human health and wellbeing as water is one of the most important resources for life on the Earth. High water quality is indispensable since tainted or polluted water can create serious health problems and environmental challenges. [5] A major worldwide problem with profound consequences is water scarcity. Rapid population increase, climate change, and unsustainable water use practices, result in the lack of fresh and clean water in

many areas of the world. [6] In addition to posing a threat to access to clean water, this situation also affects ecosystems, agricultures, and industries, particularly for drought-prone regions are at higher risk. To create safe water sources and address the global water scarcity, relevant sustainable water management practices, conservation measures, infrastructure investment, and international cooperation should be involved.

Drinking contaminated water can result in gastrointestinal troubles, waterborne illnesses, and long-term health issues. [7] Organic compounds are substances with a carbon basis that can come from both natural and artificial sources. Concern can arise when organic chemicals from poor waste disposal, industrial discharges, or agricultural runoff find their way into drinking water supplies. Potential toxicity and environmental persistence are two of the key problems with organic pollutants. This work mainly focuses on the overview of 2-methyl-isoborneol (MIB) and geosmin (trans-1,10-dimethyl-trans-9-decalol) as they are often found in water together as algal byproducts. The history of studying MIB and geosmin dates back half a century ago, when geosmin was first discovered as a by-product of cyanobacteria by Safferman in 1967, followed by the discovery of MIB by Tabachek and Yurkowski in 1976. [8] MIB and geosmin both are soil-based odorants, but their effects are mainly studied as a cause of odor outbreaks in surface waters. They are basic derivatives of terpenes produced as secondary metabolites by actinomycetes and cyanobacteria like species of oscillatoria, phormidium, planktothrix, and streptomyces. These microorganisms synthesize and store these compounds in their cell membrane. When under stress or upon their death, their cell membranes are ruptured, and these compounds are released to the water body. They give away an earthy or musty odor to the water they are in contact with and are effective as strong odorant even in ng/L levels. As a result, MIB and geosmin have been identified as the main taste and odor issue-causing compounds in drinking water [9] Although MIB and geosmin are not dangerous (non-toxic) at low quantities (at 10 to 100 ng/L concentrations), their existence in drinking water can cause a series of negative consequences on both the

aesthetic quality of the water and the general sense of water safety besides of unpleasant odors. [10]

1.2 Challenges in Detecting 2-Methylisoborneol

MIB ($C_{11}H_{20}O$) is a monoterpene compound with a boiling point of $208.7 (+/-) 8.0$ °C (Fig. 1a). The molecular weight of MIB is 168.28 g/mol and a solubility in water is 194.5 mg/L. The compound is not recognized as any kind of irritant or otherwise at any concentration. It is expected to have a vapor pressure of 6.68×10^{-5} atm. The (-) MIB is a naturally occurring enantiomer. Compared to the (+) MIB, they both share the same characteristic of being an odorant but the (-) MIB has the higher potential of smell and taste. Also, the (-) MIB has a lower OTC (Odor Threshold Concentration), being 10 times lower than the (+) MIB. It has a similar occurrence pathway as geosmin but involves geranyl diphosphate (GPP) methylation and subsequent cyclization to 2-MIB in cyanobacteria from (E)-2-methylgeranyl diphosphate (2-MeGPP) by methyltransferase gene and monoterpene cyclase gene, respectively. The main step involved is the terpene cyclization. The OTC of MIB is 9 parts per trillion (ppt) or 9 ng/L in water [11].

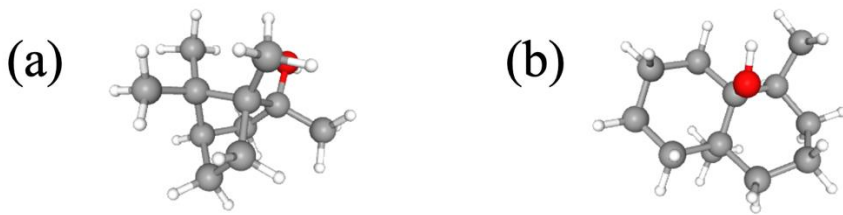


Figure 1: Chemical structure of (a) MIB and (b) geosmin.

The incredibly low detection level causes difficulty for the detection of the compound in water samples without the use of expensive equipment or thorough laboratory training. The current most common detection method of detection for 2-MIB and geosmin is solid phase micro extraction, which requires the testing of an individual sample by a trained professional [12]. The prospect of an in-situ, sensitive

detection method for use in drinking water flow can allow for the constant regulation and knowledge of any taste and odour compound present without the need for further testing.

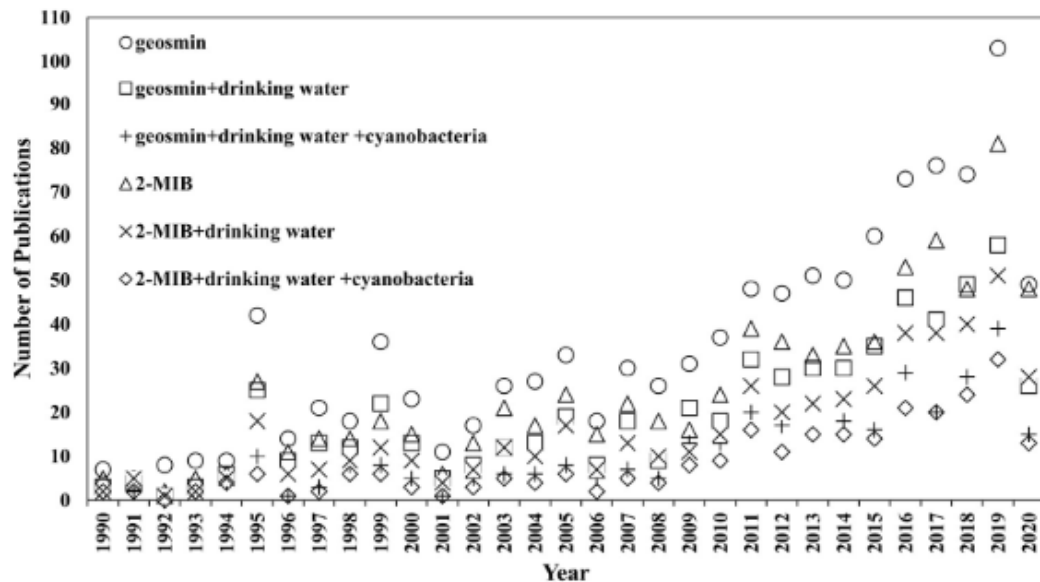


Figure 2: Number of publications per year on geosmin and 2-MIB based on a literature search (Scopus) depicting the relevance of geosmin/ 2-MIB events over the years (1990-June 2020) [2]

Figure 2 highlights the extent to which taste and odour compounds are now understood to be a predominant issue in regards to public perception of tap water, with 2-MIB and geosmin being identified as the leading compounds. 2-MIB and geosmin have a very similar chemical structure, due to this, detection methods which are less selective to minor changes in their structure can miscalculate concentrations of one due to the detection of the other in the same sample, which is common in uncontrolled water samples.

Standards for cyanotoxins or total cyanobacterial cell count have been established by many institutions, which may accidentally address the problem of MIB and geosmin in drinking water. These recommendations are meant to safeguard the general people from any potential health concerns brought on toxic cyanobacterial blooms and their consequences. It is worth noting that exact recommendations may differ from one area to another, and authorities may update their recommendations for cyanobacterial

toxins, including MIB and geosmin, based on the most recent scientific research. Odor threshold concentrations for MIB and geosmin have been reported ranging from 2 to 15 and 4 ng/L, respectively. [13-15]

The biosynthesis of both MIB and geosmin have been studied thoroughly and it has been demonstrated that there are multiple pathways for biosynthesis of these compounds. Several different biosynthesis pathways of isoprenoid synthesis that exist in microorganisms, one or more of which may lead to the production of geosmin by different taxa. The pathway which has been found to be the major biosynthetic isoprenoid route is the MEP pathway, which was discovered more recently than others. While there is evidence that the second most common pathway, the mevalonate (MVA), is also used. [16] The pathway for the synthesis of geosmin involves a specified gene from cyanobacterial organisms and is controlled by the geosmin synthase gene (*geo*), from the conversion of a single protein to farnesyl diphosphate (FPP) into germacradienol, which is then converted into geosmin. The main occurrences of geosmin day to day are in beetroot and wine. In beetroot, geosmin gives it the earthy taste and smell, while in the wine it becomes a byproduct of the fermentation process which influences the final quality. Geosmin in stagnant waters provides a favourable condition for the existence of yellow fever mosquitos, which also provide favourable conditions for geosmin. This effect is due to eggs of mosquitos in a geosmin rich body of water allowing for the algae production, which bacteria will then use to disperse themselves for growth further spreading the effect of algal bloom. This has been shown to have pathogenic effects on human beings.

Although these two compounds have not been associated with any serious health effects, the resulting taste and odour from their presence in the water is perceived as unsafe by consumers and cause them to switch their drinking water from tap to bottled. This problem is acute in summer months when cyanobacterial blooms are common due to warmer, nutrient rich conditions. Some countries set a guideline value as 10 ng/L in their drinking waters. [17] However, studies have found that they are extremely difficult to remove by conventional water treatment methods due to the

tertiary alcohol structure of both MIB and geosmin. Since MIB and geosmin are considered as key indicators of water quality by consumers, it is imperative to monitor their level in various water sources. This review will cover the history of research into the detection methods of both MIB and geosmin, as well as look into the most recent technological developments in the area, allowing for new detection methods to be introduced.

1.3 Research Objectives

The primary objective of this research, due to both customer complaints and the public opinion on drinking water, is the production of a sensor with a detection limit lower than that of human detection levels. The development of an electrochemical biosensor for the in-situ, sensitive detection of MIB in drinking water systems to replace current detection techniques would allow for a greener detection process, while being cheaper for industry. The project was developed in partnership with Welsh Water, and the use of a molecularly imprinted polymer (MIP) was identified as the basis of the research, given the potential and lack of knowledge on the subject area. This will be achieved through the testing and optimization of a range of parameters within the polymer itself, as well as the sensor base.

Initially, a literature review was completed on the premise of the detection of MIB, including, but not limited to that of electrochemical biosensing. This allowed for the understanding of both the relevance and importance of this research, in an area where the need for in-situ and sensitive detection is critical to ensuring the public perception of drinking water is maintained as positive. The review highlighted the lack of research into the use of an MIP on MIB, as they are a relatively recent premise, however, have proved to be incredible sensitive and efficient in other aspects of life and industry.

The primary focus of this research individually is the design and testing of the polymer itself, which involved optimising the parameters of the production and utilisation of the sensor. This paper includes the optimization of the volume of MIP, the solution used for template removal, the time of template removal and the time of reintroduction of the template molecule. The volume of the MIP will be optimized through obtaining cyclic voltammetry profiles on the sensor before and after the application of the MIP at different volumes. The solution used for template removal is an area of research which is underdeveloped regarding solution efficiency for varying target molecules. This led to different solutions being tested and compared based on electrochemical impedance spectroscopy (EIS) results from analysing both the Bode and Nyquist plots on both MIP and non-imprinted polymer (NIP).

The sensitivity and selectivity of the sensor will be tested once the polymer and sensor itself has been fully optimised. This is done using a range of controlled concentrations of MIB present in deionised water, which will be tested through EIS and analysed against different increments of concentrations to determine an overall profile of the change in current of the sensor based on the known concentration of MIB in the sample. This allows for future, uncontrolled samples to be tested and placed on the profiling graph to understand the concentration which is present in the sample.

1.4 Environmental Impact and Technological Advancement

The conclusion of this research would allow for the placement of these sensors within set locations in water pipes themselves, with the potential to be connected to a computer remotely, giving constant concentration updates throughout the system. This would allow for the concentration to be controlled and regulated remotely, as well as a better understanding of the MIB levels at all stages of the purification process.

The sensors themselves would be incredibly cost effective for industry compared to the current techniques used for detection, as well as remove the need for training of use, instead all that would be required is the understanding of the implementation and installation of the sensor, along with the understanding of the graphical information.

The potential of the use of a carbon- based sensor made from waste coffee grounds within the research group allows for the sensor itself to be environmentally friendly, while also removing and recycling waste coffee grounds rather than them being a burden environmentally. The in-situ nature of the sensor would allow for the removal of travel times in the detection stages and remove the use of larger equipment or potentially wasteful chemicals during the detection process. The chemicals used in the polymer synthesis are low volumes and any waste is disposed of in the correct manner. The increased presence of MIB in the water can also be harmful to aquatic life in the area, meaning the sensors could be used to understand and regulate the concentration of MIB in natural water sources.

Chapter 2 Literature Review

2.1 Chromatography-based methods for detection of MIB and geosmin

Initially, chromatography-based methods for water analysis such as gas chromatography and mass spectrometry (GC-MS) along with a variety of effective preconcentration approaches and high-performance liquid chromatography-mass spectrometry (HPLC-MS) were approved by water agencies worldwide to achieve high-performance detection of MIB and geosmin. The accuracy of these methods is critically dependent on the nature of water sample.

2.1.1 GC-MS

The GC-MS method is the combination of gas chromatography (GC) and mass spectroscopy (MS). GC is the most common analytical technique used to identify and quantify chemical compounds within a complex mixture, with a superior capacity to detect trace volatile organic compounds in water [18]. The instrument of GC contains a coiled tube filled with a gas (typically helium or nitrogen) as the mobile phase and a liquid as the stationary phase. Organic compounds are vaporized and transported through the column by the carrier gas at various speeds when the sample is injected into the column. Separations of compounds throughout the column are realized due to interactions between the gas and different components in the sample.

Subsequently, each separated compound enters MS and is ionized in a flame ionization detector, yielding charged particles of ions. These ions then enter a mass analyzer where they are sorted out using a magnetic field according to their mass-to-charge ratios (m/z). MS provides a list of produced ions of compounds detected. [19] Up to date, GC-MS is still widely utilized because of its capacity to separate, recognize, and measure a wide variety of volatile and semi-volatile molecules in complicated mixtures. It is indeed a useful instrument for analyzing compounds both

qualitatively and quantitatively. As these compounds need to be determined at very low concentrations, a preconcentration method is often required.

Table 1: GC-MS along with different preconcentration techniques for detection of MIB and geosmin.

Method of Detection	LOD of geosmin (ng/L)	LOD of MIB (ng/L)	Ref.
SCLSA-GC-MS	0.8	0.8	[20]
CLSA-GC-MS	0.1	1	[21]
CLSA-GC-LRMS	2	2	[22]
CLSA-MSRT-GC-MS	4	4	[23]
CLSA-GC-FID	4.97	5.2	[24]
HFSA-GC-MS	1.8	2.2	[25]
ME-GC-ITD-MS	1	1	[26]
LLME-GC-MS/MS	0.2	1.2	[27]
DLLME-GC-MS/MS	0.5	1	[28]
SPME-GC-CI/EI-ITMS	0.8	0.9	[29]
HS-SPME-GC-MS	0.5	0.7	[30]
HS-SPME-GC-MS	3.3	1.2	[31]
HS-SPME-GC-MS	0.3	0.6	[32]
SPME-GC-ITMS	0.48	0.34	[33]
HS-SPME-GC-MS	0.6	0.9	[34]
PPG coated HF membrane	4	9	[35]
HS-SPME-GC-MS	10	15	[36]
HS-SPME-GC-MS	0.58	0.25	[37]
HS-SPME-GC-MS	0.4	0.6	[38]
HS-SPME-GC-MS	1	1	[39]
HS-SPME-GC-MS	0.44	0.35	[40]
HS-SPME-GC-MS	0.29	0.46	[41]
HS-SPME-GC-MS	0.67	0.45	[42]
VA-HS-SPME-GC-MS	1.7	2.5	[43]
HS-SPME-GC-MS	0.04	0.13	[44]
HS-SPME-GC-MS	0.2	0.5	[45]

HS-SPME-GC-FID	10	10	[46]
HS-LPME-GC-MS	1.1	1	[47]
SPE-HS-GC-MS	0.0001	0.0001	[48]
SPE-GC-MS	0.5	0.5	[49]
SPE-GC-MS/MS	0.9	5.5	[50]
SPE-LVI-GC-MS	0.63	0.91	[51]

Reports on detection of MIB and geosmin based on GC-MS along with a variety of preconcentration approaches are presented in Table 1. Closed-loop stripping analysis (CLSA) has been widely used for the analysis of non-polar volatile organic compounds (VOCs) of intermediate molecular weight at the ng/L to μ g/L level. This method can be applied to both raw and treated waters. It is the first standard for isolation or preconcentration of MIB and geosmin, with the limit of detection (LOD) usually reported as 1 ~ 2 ng/L. [13] According to LODs of MIB and geosmin, this method seems to be not very sensitive when it coupled with other techniques like the multichannel silicone rubber trap (MSRT) [23] and flame ionization detection (FID). [24] Low-resolution mass spectrometry (LRMS) was demonstrated that it was not able to provide a lower minimum detection limit as the MS. [22] Interestingly, two reports of using the CLSA-GC-MS and salted closed-loop stripping analysis coupled to gas chromatography-mass spectroscopy (SCLSA-GC-MS) presented relatively lower LODs of MIB and geosmin at around 1 ng/L. [20, 21] Hollow fiber stripping analysis (HFSA) is another classic method for analytic extraction of odor producing compounds. [25] The HFSA used microporous hydrophobic hollow fiber membranes for the analysis and can measure ppt concentrations in water. However, the apparatus setup of the HFSA is complex and involves a large amount of equipment. The extraction or preconcentration time is much longer about 90 ~ 120 min. Bao et al., applied microextraction in combination with gas chromatography-ion trap detection-mass spectrometry (ME-GC-ITD-MS) to detect odorous compounds, with LODs of MIB and geosmin reached at 1 ng/L, indicating the improved GC-MS could offer slightly better results than the HFSA preconcentration. [26] Liquid-liquid micro-

extraction (LLME) is also a prevalent approach for detection of MIB and geosmin. Dispersive liquid-liquid micro-extraction (DLLME) is a new micro-extraction technique. It is promising because of the simpler operation and less extraction time, which calls for the method to be further researched. This class of preconcentration method usually integrates with the gas chromatography tandem mass spectrometry (GC-MS/MS). [27, 28] The LOD of MIB obtained from the LLME-GC-MS/MS and DLLME-GC-MS/MS, however, were not as sensitive as that of geosmin.

Solid phase micro-extraction (SPME) is an effective method used to measure organic micropollutants, especially VOCs. It is simpler and more cost-effective than the CLSA, leading to an increase in its popularity. [52] Headspace solid phase micro-extraction (HS-SPME) have been widely used over other preconcentration methods [30, 32, 34, 37, 38, 40-42, 45]. It often produced sensitive results for both MIB and geosmin when coupled to the GC-MS, except a few reports in which LODs were higher than 1 ng/L. [31, 36, 39] Liu et al., constructed a passive sampling device consisting of hollow fiber (HF) membranes coated with polypropylene glycol (PPG) for field equilibrium sampling of MIB and geosmin (Fig. 3a). [35] The reported strategy presented LODs of 9 and 4 ng/L for MIB and geosmin, respectively. The values were slightly lower than their OTCs, but still had room for further improvement. Furthermore, several studies have been carried out to optimize the SPME for analysis of MIB/geosmin in water such as vacuum assisted headspace solid-phase microextraction coupled to gas chromatography-mass spectrometry (VA-HS-SPME-GC-MS) (Fig. 3b) [41], headspace liquid-phase microextraction coupled to gas chromatography-mass spectrometry (HS-LPME-GC-MS) [47], yielding competitive LODs as well. Flame ionization detection (FID) is simpler and much more cost-effective than the MS and are therefore more easily accessible to the wider scientific community. The FID measures the current produced from burning of organic compounds by a hydrogen-air flame. The current generated is proportional to the amount of sample being burnt. However, the separation and purification for the

targeted sample are often required and using this method to achieve the specific identification of compounds is not very reliable. Although the FID is more cost effective than the MS, it is not as functional in result. [46] Electron ionization (EI) is used when results are within the extensive fragmentation range. [53] For this method to be successful, very high purity of the sample of analysis must be maintained for the spectrum to be free of background noises, even simple contaminants can cause heavy changes in the spectrum. The analysis of MIB and geosmin through the EI is not feasible as multiple background noises will be produced if the raw water sample is directly analyzed, thus destroying the spectrum. However, if the EI is used with an extraction method, the result yielded has shown to be very promising. Chemical ionization (CI) uses a lower input of internal energy into the sample. This method makes use of gas phase chemical reactions to ionize the sample, making fragments are simple, and the identity of the molecule is traceable. Though right reagent for the CI has been selected to be able to provide as clear the spectrum as the EI, the peak intensity is still not greater than the EI spectrum and no further studies are proceeded in the CI. McCallum et al., integrated the SPME with a developed MS of chemical ionization/electron impact ionization-ion trap mass spectrometry (CI/EI-ITMS) for sensitive screening of MIB and geosmin [29], and another similar application of the ITMS was claimed by Sung et al. [33], they both achieved comparable LODs below 1ng/L. Peng et al., evaluated factors affecting the HS-SPME-GC-MS via an orthogonal design study, and reported highly improved LODs of 0.13 and 0.04 ng/L for MIB and geosmin, respectively [44]. The analytical procedure regarding solid-phase extraction (SPE) is simple as this method can be performed without solvent extraction. Several studies on the analysis of MIB and geosmin using GC-MS [49], GC-MS/MS [50], as well as large volume injection (LVI)-GC-MS [51], with the preconcentration of SPE have been reported, along with sensitive LODs below 1ng/L. The use of LVI-GC-MS enabled MIB and geosmin to be detected within a dynamic range of 0.5 ~ 20 ng/L, along with chromatographic variation of these two compounds evaluated by GC-MS (Fig. 3c). Ikai et al., combined the SPE with headspace gas chromatography-mass spectrometry (HS-GC-MS), and achieved an

ultralow LOD of 0.0001 ng/L for MIB and geosmin. [48] It is considered as the lowest LOD provided in comparison to other reports.

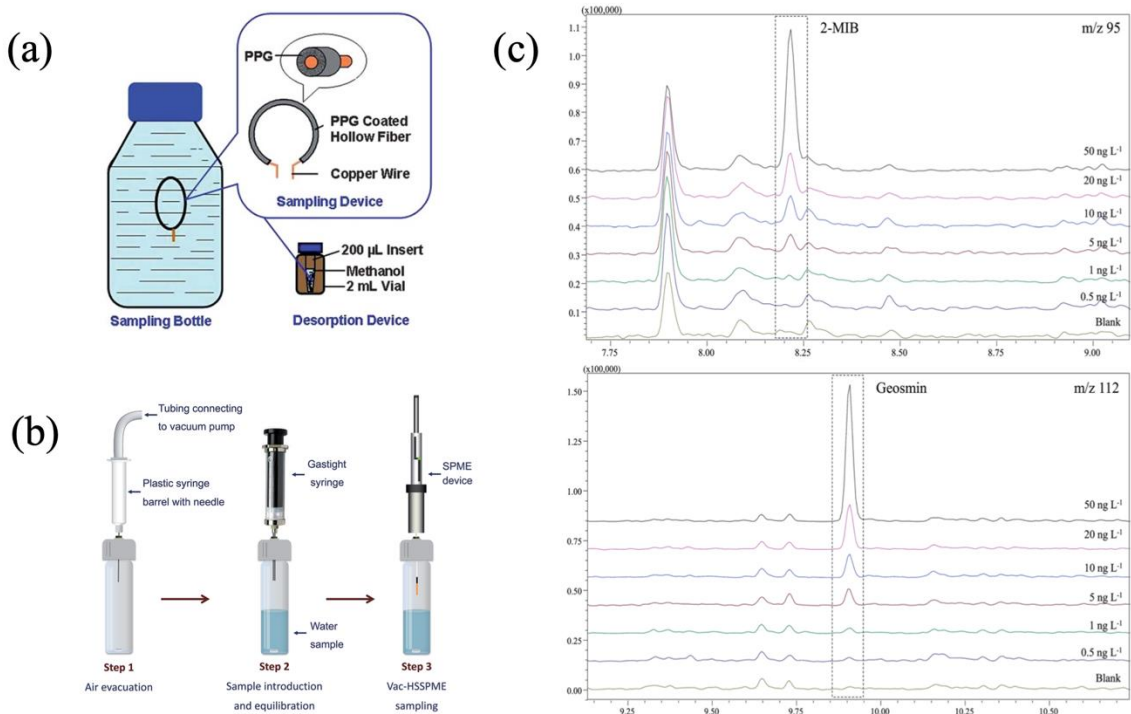


Figure 3: (a) Schematic representation of the passive sample device for detection of MIB and geosmin. Reprinted with the permission of [35]; (b) Schematic illustration of the vacuum-assisted headspace solid-phase microextraction (VA-HS-SPME) assemble. Reprinted with the permission of [51]

The method of ion mobility spectrometry (IMS) is still under development to be used as a detector. Differential mobility spectrometry (DMS) was used in combination with headspace gas chromatography (HSGC) to identify several VOCs including MIB and geosmin. [53] This method detects the concentration of organic compounds well below their OTC levels but is only used in the raw wine sample. If this method is developed further especially by factoring in water parameters for the OTC detection in raw water samples, it would really have the potential to replace the MS and to be one of prime detection methods for MIB and geosmin. Further development is needed to couple IMS with MS to provide even better standard analysis for MIB and geosmin. For example, field assisted ion mobility

spectrometry-mass spectrometry (FAIMS-MS) could be a very good alternative to the conventional GC-MS, as it is more cost effective and compact than the GC.

2.1.2 HPLC-MS

HPLC-MS is another effectively analytical technique used to identify and measure chemicals in complicated samples, including water. [19, 54] A liquid mobile phase (i.e., an organic solvent/water mixture) and a column carrying a nonpolar liquid stationary phase are used in the analytical method known as HPLC. Organic molecules are detected using absorbance detectors, while metallic and inorganic substances are detected using conductivity or electrochemical detectors. Atmospheric pressure chemical ionization (APCI) and electrospray ionization (ESI) are commonly ionization techniques applied in HPLC, as they produce protonated molecular ions $[M+H]^+$, which are frequently employed for quantification. Same as GC-MS, MS is used for identifying the eluent from the HPLC column with great sensitivity and selectivity. Standard solutions and calibration curves are used to calculate the amount of targeted compounds in presence of the water sample. The data collected from the HPLC-MS is usually analysed through a sophisticated software, yielding results of the concentration of compound detected in the water sample.

2.2 Colorimetric Methods for detection of MIB and geosmin

Chemiluminescent reactions are carried out based on the luminescent reaction which is a quantifiable intensity measurement of molecules under discussion. Hydrogen peroxide mixed with potassium peroxy di-sulphate ($K_2S_2O_8$) or luminol is the reagent used for the chemiluminescence reaction measurement in the detection of MIB and geosmin. The concentration of reagents is optimized with respect to the intensity of the chemiluminescent reaction, the difference in the concentration of $K_2S_2O_8$ before and after the completion of chemiluminescent reaction is consumed for the oxidation

of MIB and geosmin. [55] Enzyme linked immune-sorbent assay (ELISA) is a technique of antibody-antigen based binding analysis. Like other methods, this process involves a dehydrated product of geosmin, 4, 4a, 5, 6, 7, 8-hexahydro-4a-methyl-2(3H)-naphthalenone, as the selection of the antibody, which is extracted from goat serum. However, a poor detection limit of 1 $\mu\text{g}/\text{L}$ makes commercial applications of the ELISA difficult without an extensive pre-concentrating step beforehand. An ELISA assay containing a polyclonal antibody (pAb) for detection of MIB presented a LOD of 4,800 ng/L, along with an IC₅₀ of 105,000 ng/L, which was far beyond the prescriptive OTC. [56] Future work is required to provide an ELISA with a LOD below the OTC of human, and the development of a more selective antibody for geosmin binding could lead to the adoption of ELISA testing for routine detection of geosmin in water. Other methods such as bromine reaction was also used for determination of geosmin. In 1990, a modified reaction of Tortelli-Jaffe Reaction was first employed. However, this method is merely suited for the detection of geosmin at higher concentrations and is only specific to a dehydrated diene version of geosmin. Therefore, this reaction is only applicable to geosmin but not MIB. [57]

2.3 BMD from US-EPA

The U.S. Environmental Protection Agency (EPA) uses a variety of analytical techniques and benchmarking strategies for evaluating and regulating environmental issues. Among them, the Benchmark Dose (BMD) approach is one of well-known analytical techniques approved by the EPA. In the context of risk assessment for chemicals and environmental contaminants, the BMD method is a statistical technique used to determine the dose or concentration of a substance that can cause a specified level of detrimental consequences. This strategy is especially helpful in dealing with non-linear dose-response relationships and low-dose extrapolation. [58] It enables EPA to establish reference doses or concentrations for a wide set of

compounds and set safe limits of exposure. Thus, the BMD approach is regarded as a more reliable and scientifically sound way for determining health hazards connected to exposure to environmental toxins.

These traditionally analytical methods can provide high-performance detection towards water pollutants such as MIB and geosmin. However, there are also some limitations that hinder their further applications. For example, highly expensive instruments used in GC-MS and HPLC-MS, which require professional instruction prior to operation. Also, regular maintenance upon the instrument is compulsive to make sure it works under qualified conditions. Moreover, the large outline of the instrument makes these methods not suitable for real-time water monitoring or other portable uses. Although the BMD method offers reliable threshold concentration values for a broad range of toxic substances, it only can be performed by authorized laboratories. Therefore, there is still a necessity to develop low-cost, simple, highly accurate, and portable sensing platforms (e.g., sensors or biosensors) for ultra-sensitive detection of water pollutants at nano-level concentrations or even lower.

2.4 Sensors used for detection of MIB and geosmin

The ability to detect odorous compounds in water on site and effectively without the use of previously necessary lab techniques is highly promising for the water treatment industry, allowing non-specialised technicians to determine their concentration in a solution. With presence of biological recognitions on the electrode, target molecules can bind with them to allow the electrode to create electrical signals, allowing for odorous compounds to be detected at previously unachievable levels, without the use of off-site lab techniques. Sensors for the detection of MIB and geosmin including several subclasses ranging from electrochemical sensors to

electronic tongues or noses, along with various functional or bio-functional modification upon electrode surfaces are compared in this review, as seen in Table 2.

Table 2: Determination of MIB and geosmin based on sensing methods.

Target pollutants	Recognition elements of electrodes	Detection methods	LODs (ng/L)	Refs.
MIB	MIB-imprinted polymer	QCM	10^4	[60]
Isoborneol	Gold electrodes screen printed onto AT-cut crystal sheets coated with isoborneol-imprinted polymer solution	QCM	8.95×10^7	[61]
MIB and geosmin	Interdigitated gold microelectrodes coated with ultra-thin polymeric films	Electronic tongue with impedance	25	[69]
Isoborneol	Nylon 6,6 and chitosan electrospun nanofibers reinforced by cellulose nanowhiskers united with functional nanoparticle materials of AgNPs, AuMPs, and rGO	Impedimetric electronic tongue	< 25	[70]
MIB and geosmin	Human olfactory receptor and SWCNT FET	Bio-electronic nose	10	[67]
MIB	Cross-linking reagent of poly(4-vinylphenol) in thin-film transistors	Electronic nose	$< 10^7$	[68]
Geosmin	Platinum nanocarbon (Pt-Nc) film electrodes with different Pt concentrations formed by co-sputtering with UBM		100	[64]
Geosmin	Geosmin-imprinted polymeric membrane layered on the surface of the GCE via the electrochemical deposition method	CV	5	[63]

2.4.1 Quartz crystal microbalance (QCM) sensors

QCM sensors are a class of mass-based sensors measuring the change of frequency related to chemical or bio-chemical events on piezoelectric platforms such as quartz. [59] For determination of MIB and geosmin, QCM sensors are often applied with surface functionalization of molecular imprinted polymers (MIPs). Ji et al., fabricated a QCM sensor where the MIP was made up using MIB as the template, methacrylic acid as the functional monomer, ethylene glycol dimethacrylate as the crosslinker, and 2,2'-azobis (2,4-dimethyl) valeronitrile as the initiator. [60] This MIP solution was pipetted in five microlitre layers onto each QCM and polymerized at 40°C for 48hr in nitrogen-purged and sealed glass vials. In this test, non-imprinted samples were created using the same method as the imprinted simply without the inclusion of the template MIB. The sensors were all then washed in ethanol and dried to remove the template from the imprinted sensors. The potential of this method is shown throughout research as it has allowed for the selectivity of the sensor to be improved 20-fold while maintaining selectivity. This means the detection limit of the non-imprinted polymer to the molecularly imprinted polymer (MIP) changes from 200ppb to 10ppb. The experiments show that the sensitivity of this sensor when detecting other compounds such as geosmin or other cyanobacteria is significantly decreased due to the imprint, although this was expected prior to testing. Another sensor selective to isoborneol in water samples was developed where the sensing layer of molecularly imprinted polymers was deposited onto transducer surfaces and quartz crystal microbalance (QCM). [61] The analysis showed that an increase of isoborneol concentration was associated with a linear decrease in the frequency response of the sensor. This is attributed to a greater number of molecules binding to the surface of polymeric layers. Moreover, the response time of the fabricated imprinted polymer sensor is 90 s in the high concentration of isoborneol (e.g., 5 mM) and 60 s in the low concentration (e.g., 1 mM). The increase of isoborneol concentration causes a higher binding rate to specific cavities and therefore takes more time to assure a stable signal compared to lower concentrations. The fabricated sensor, consisted of gold electrodes screen printed onto AT-cut crystal sheets of 10 MHz coated with analyte-imprinted polymer solution, was able to detect isoborneol

ranging from 1 mM to 5 mM, with a theoretical detection limit of 0.58 mM or 8.95×10^7 ng/L.

2.4.2 Electrochemical sensors

Due to the complexity of chemical analysis, especially for very low concentrations of pollutants, electrochemical sensors have been developed for the identification of toxic substances to monitor the water quality. Electrochemical sensors normally consist of a receptor and a physicochemical transducer (Fig. 4). The receptor can be fabricated as activated or macro-molecular surfaces that cause considerable specific interactions with the pollutant, aiming to interact the chemical recognition layer (i.e., coated on a transduction element) with the target analyte and convert this event into a quantifiable output electrical signal. [62] A successful receptor can maintain a high level of analyte specificity in presence of various interfering chemicals. Transducer has the responsibility to convert output signals from the receptor into readable values to be displayed. There are mainly three types of electrochemical transduction including the potentiometric, amperometric, and impedimetric transduction. Integrated with a signal processing system, electrical signals are modulated into a form that is accessible and readable.

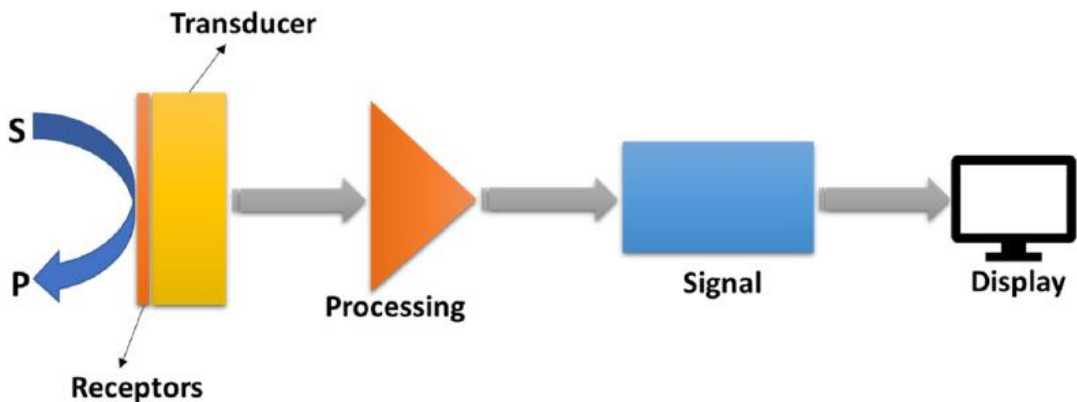


Figure 4: Components of a general electrochemical sensor. Reprinted with the permission of [62].

Specifically, potentiometric sensors are the most widely used due to its cost and simplicity. The potential difference between a reference and a sensing electrode is

usually measured in this type of sensors. As the sensing electrode interacts with MIB and geosmin, the shift of potential occurs and is immediately translated into a voltage signal that can be measured, which is logarithmically proportional to the concentration of analytes. For the amperometric detection, a steady voltage is applied to the working electrode, serving as a driving force for electrocatalytic redox couples that produces an electrical current related to the concentration of analytes. In the determination of MIB and geosmin, the oxidation or reduction of analyte molecules at the electrode surface causes a current which is proportional to their content in the water sample. The resistance to the flow of an alternating current (AC) through the electrode-electrolyte interface is measured by impedimetric or conductometric sensors. These sensors measure changes in the surface impedance to quantify analyte specific recognition events on the electrode, revealing information about the analyte concentration.

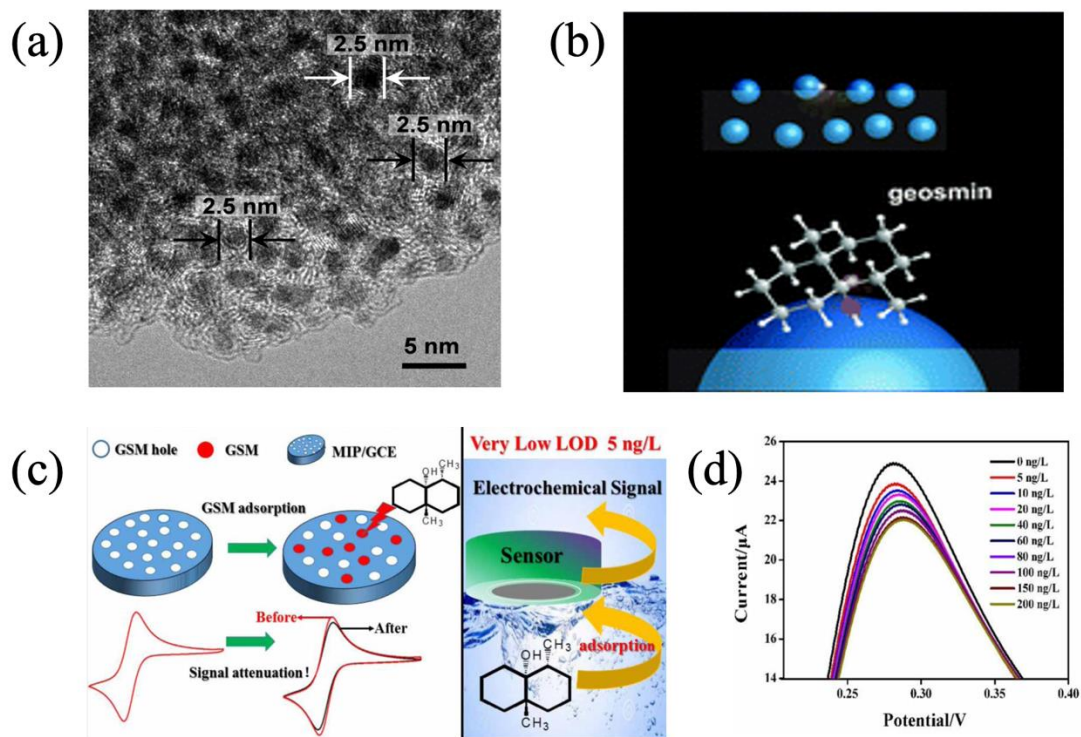


Figure 5: (a) The TEM image of nanoparticle-embedded nanocarbon film (Pt-Nc). Reprinted with the permission of [64]; (b) The use of the Pt-Nc film for detection of geosmin. Reprinted with the permission of [64]; (c) The geosmin-imprinted polymer-based electrochemical sensor used for determining geosmin in water. Reprinted with the permission of [63]; (d) CV variations in regard of different geosmin concentrations ranging from 5 to 200 ng/L. Reprinted with the permission of [63].

An electrochemical sensor based on the GCE was synthesized for determination of geosmin in water specimens (Fig. 5c). [63] The modification of MIP on the electrode surface was carried out using electrochemical deposition method. The cyclic voltammetry (CV) is applied to characterize the electron transfer of the electrode by using potassium ferricyanide as a redox couple. Geosmin molecules recognized the binding sites of the polymer matrix, forming steric resistance against the redox probe towards the electrode surface. This allows for the concentration of geosmin to be directly proportional to the decrease in electrical signals measured by the electrochemical deposition (i.e., the MIP). The proficiency of the electrochemical sensor was assured due to its capacity to detect geosmin in the range of 5 ~ 200 ng/L, offering the lowest detection limit of 5 ng/L (Fig. 5d). Kamata et al., electrochemically detected geosmin using platinum-nano carbon (Pt-Nc) film embedded electrodes. Pt with different concentrations (4.8 ~ 35.9 at%) was deposited via co-sputtering with unbalanced magnetrons (UBM) (Fig. 5a, b). The comparison among the developed Pt-Nc, nano carbon only, and sputtered Pt film without nano carbon was performed to testify the superiority of the Pt-Nc film functionalized electrochemical sensor. In the presence of peroxide (H₂O₂), the Pt-Nc film electrode showed the highest electrode activity against geosmin, compared to that of the electrode coated only with the Pt film. Accordingly, the Pt-Nc film electrode detected geosmin at lower concentrations than the Pt film electrode. This improved performance may be due to the oxidation property of Pt towards geosmin. In this regard, the detection range of geosmin yielded was 0.1 ~ 1,000 µg/L, with a detection limit of 100 ng/L. [64]

2.4.3 Electronic tongues and noses

Gas sensor arrays and liquid sensor arrays known as electronic noses and tongues, respectively, are often used for screening of MIB and geosmin in recent years. The use of such electronic sensing has been widely studied due to their ease of use and in-situ ability. The gas sensor arrays work through analysing the response patterns with pattern recognition routines and/or chemometrical methods in an array of bio- or chemical- sensors. Signals produced by gas sensor arrays are not specific to a

chemical compound in the water being tested, however, this signal pattern can be used to assess the water quality. These signals when used in a software can be related to individual samples to recognize the compound correlated to the response pattern. [65] Initial research into electronic sensing was the use of electronic noses for detection of various odorous compounds such as MIB and geosmin in water. Nonetheless, it was found that natural factors such as humidity and temperature affected the result gathered. Facing this challenge, electronic tongues are seen as a potential solution due to humidity taking a secondary role. An “electronic tongue” or a taste sensor is simply used to classify qualities of food, drinks, water, and processing fluids. It works through employing chemical sensor arrays which are soaked in the test solution. This allows the sensor interface to have enhanced selectivity. [66]

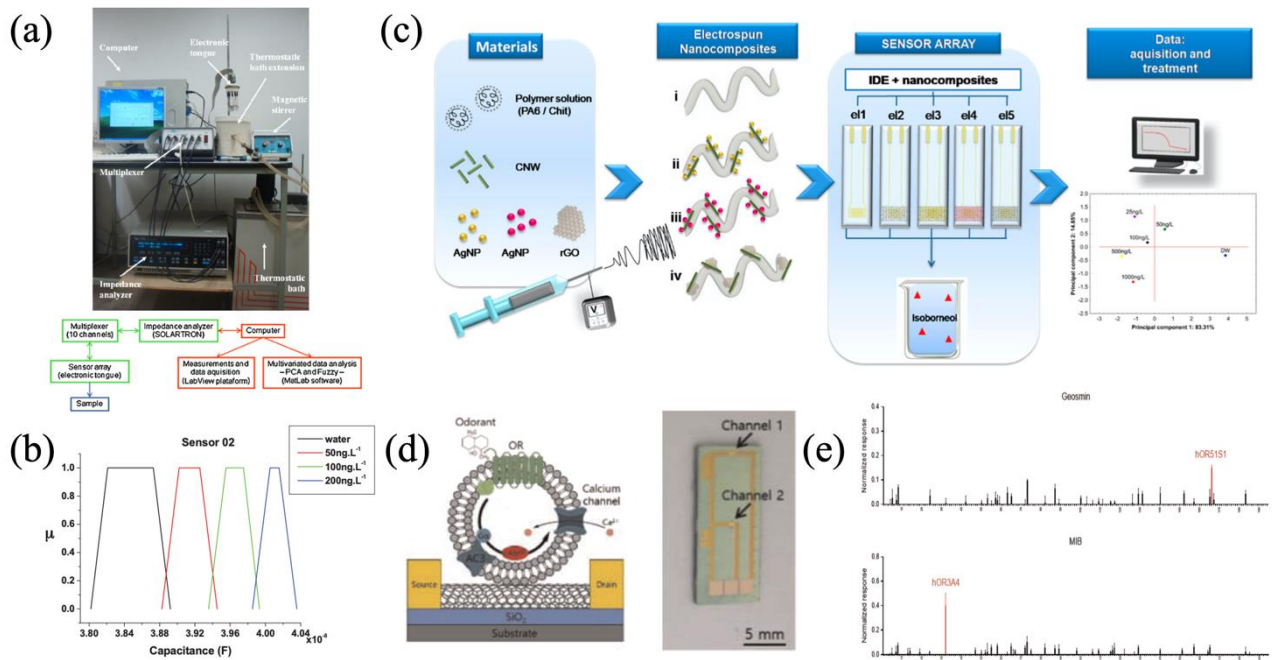


Figure 6. (a) Schematic illustration of the electronic tongue system used for detection of MIB and geosmin, along with the flow chart below. Reprinted with the permission of [70]; (b) Electrical capacitance signals in regard of different geosmin concentrations based on sensor 2. Reprinted with the permission of [69]; (c) Schematic representation of the impedance-based electronic tongue platform based on nanocomposites for the determination of isoborneol in water. Reprinted with the permission of [70]; (d) Schematic diagram of the bioelectronic nose, along with a real image. Reprinted with the permission of [67]; (e) 193

human olfactory receptors towards the detection of MIB and geosmin at 1 $\mu\text{g}/\text{mL}$. Reprinted with the permission of [67].

Son et al., prepared a bio-electronic nose with a human olfactory receptor and a single-walled carbon nanotube (MWCNT) field effect transistor (FET) for monitoring of the soil odor in water pollution (Fig. 6d). [67] The biosensor was designed with two channels of human hOR3A4 and hOR51S1 for simultaneous detection of MIB and geosmin, respectively (Fig. 6e). The interaction between the target compound and the OR caused a signal transduction with the olfactory sensing mechanism. This resulted in an influx of Ca^{2+} ions into the nanovesicles, providing a field effect. The lowest limit detection of MIB and geosmin was 10 ng/L under optimally experimental conditions. These results were obtainable without any pre-treatment required, as well as, simultaneously between the two compounds. García et al., developed a gas sensor of an organic low-cost electronic nose of thin-film transistor with a high selectivity to isoborneol. [68] The device constituted of interdigitated microelectrodes which were processed over flexible glass substrates, followed by introducing a cross-linked dielectric layer of poly(4- vinylphenol) to assure high compatibility between the electrode and the substrate, thus improving the semiconductor deposition. The fabricated gas sensor can be used in a step forward towards the assessment of water quality and detecting MIB in water samples. However, the detection capacity towards MIB provided by the sensor was below 10 ppm or 10^7 ng/L. This value is much higher than that presented by Son et al., indicating further development is required to improve the device sensitivity. Integrated with impedance measurements and multivariate data analysis utilizing the fuzzy logic program, Braga et al., created an electronic tongue system based on interdigitated gold microelectrodes coated with ultra-thin polymeric films to identify and quantify water samples having MIB and geosmin. [69] The polymeric films were deposited using the layer-by-layer technique with the aid of an automate deposition system. The array used was composed of 5 sensors, with each being chosen based on their better performance features individually. The electronic tongue system was composed of arrays of sensors connected to an impedance analyzer through a multiplexer which acted as a switch, allowing for interrogation of sensors with all

measurements performed at 25 °C as samples immersed in a thermostatic bath (Fig. 6a). High correlation linear fit curve was yielded relying on the capacitance data analyzed by the analog controller (Fig. 6b). The electronic tongue also showed sufficient sensitivity to recognize differences in the sample composition brought on by mixing contaminants at varying molar ratios. The LOD for MIB and geosmin measured via this system was 25 ng/L. Migliorini et al., evaluated the performance of a novel electronic tongue in which the sensing layer was fabricated by the integration of nanomaterials and electrospun nanofibers and used it to detect isoborneol at low concentrations, a chemical compound possessing a quite similar structure to MIB (Fig. 6c). [70] The electrospun was applied to increase the area/volume ratio and therefore improved interaction with the analyte molecules. Specifically, the sensor layer constitutes of nylon 6,6 nanocomposites (synthetic polymer) and chitosan electrospun nanofibers reinforced by cellulose nano-whiskers united with functional nanoparticle-based materials including silver nanoparticles (AgNPs), gold nanoparticles (AuNPs), as well as reduced graphene oxide (rGO). The integration of nanomaterials and electrospun aids to enhance the charge transference besides providing superior characteristics of hydrophilicity, biodegradability, nontoxicity, and biocompatibility and therefore enhances the selectivity of the sensor. Also, the functionality of nanofibers surface with metal nanoparticles is important to elevate the detection efficiency and nano-whiskers are used to enhance the dispersion of metallic nanoparticle materials. The novel sensor was able to distinguish contaminated water samples with isoborneol at nano-molar concentrations lower than 25 ng/L. Real water testing was also performed by using river water samples containing a certain amount of isoborneol, aiming to assess the superiority of the proposed sensor. The capability of the sensor to distinguish different concentrations of isoborneol at 1 kHz of electrical capacitance responses was eventually demonstrated according to the principal component analysis (PCA).

2.4.4 Molecularly Imprinted Polymer

The prospect of a molecularly imprinted polymer through electrochemical biosensor usage describes the use of a polymer surface for biorecognition of interactions on its

surface based on the target molecule imprinted. This process is designed to imitate enzyme interactions through the interaction of the target molecule and designed cavities on the polymer surface available for rebinding. Early MIP usage is outlined through the work of K. Mosbach and B. Sellergren [71], which reported an “imprinted polymer” in 1984, and G. Wulff’s [72] series titled “Enzyme-Analog Built Polymers” beginning in 1973.

The optimization of MIP recipe varies depending on the desired target molecule, while factors such as monomer to template ratio and initiator volume is believed to be consistent across the board. [63] Monomer to template ratio is a factor that must be taken into account to allow for the presence of selective cavities on the polymer surface, dependant on the concentration of template molecule in the recipe, while monomer concentration controls the ability of the polymer to bind to the electrode surface and polymerise effectively.

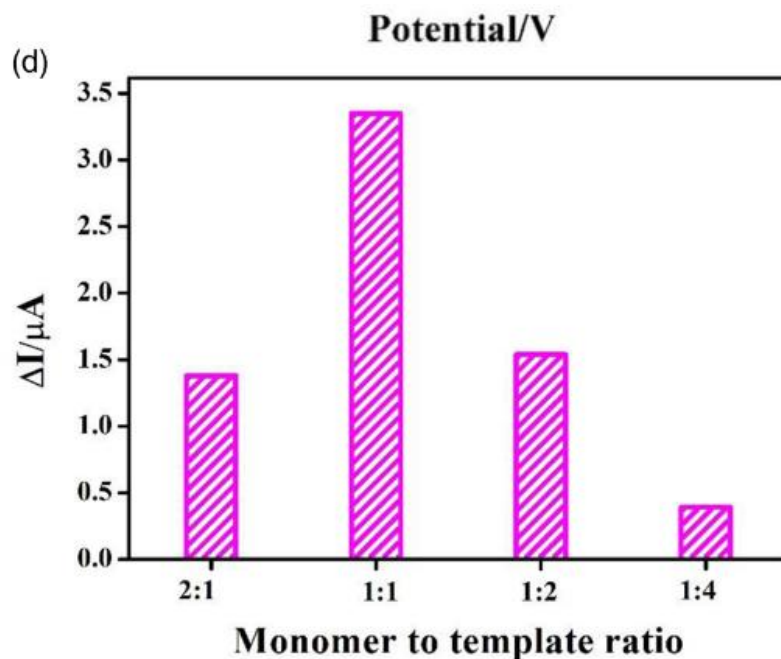


Figure 7: The effect of the ratio between template molecules and monomers using Geosmin and o-phenylenediamine respectively. [63]

Table 3 presents the variation of polymer recipe throughout literature, highlighting the importance of variation primarily in functional monomer and solvent usage depending on the desired template molecule. This is a result of the ability of both the monomer and template to dissolve completely in the chosen solvent, while the monomer must create a stable template-monomer complex. A stronger interaction and binding between the monomer and template is favoured to create a stable complex, as well as allow for a better rebinding process, however, creates more issues when selecting the most efficient solution for template removal prior to the reintroduction process.

Table 3: Compound selection for MIPs with differing target molecules and their removal solutions

Target	Functional monomer	Initiator	Solvent	Cross-linker	Reference	Removal
Cinchonidine	2-(trifluoromethyl)acrylic acid	Unknown	Chloroform/ acetonitrile	Ethylene glycol dimethacrylate	[73]	Methanol: Acetic acid (70:30)
Metronidazole, 1-(2- hydroxyethyl)-2- methyl-5-nitromidazole	Methacrylic acid	AIBN	DMF porogen solvent	Ethylene glycol dimethacrylate	[74]	Soxhlet
Bupivacaine	Methacrylic acid	AIBN	Chloroform	Ethylene glycol dimethacrylate	[75]	N/A
2,4- dichlorophenoxyacetic acid	4-[(4- methacryloyloxy)phenylazo]pyridine (MAzoPy)	AIBN	Acetonitrile	Ethylene glycol dimethacrylate	[76]	N/A
Diaminoaphthalene, phenylalanine anilide	Methacrylic acid	AIBN	Cyclohexanol, 1- dodecanol	Ethylene glycol dimethacrylate	[77]	Acetonitrile
Theophylline	Methacrylic acid	AIBN	Cyclohexanol, 1- dodecanol	Ethylene glycol dimethacrylate	[78]	Methanol: Acetic acid (4:1)
Oxacillin	4-Vinylpyridine	AIBN	ACN	TRIM	[79]	N/A
Sameridine	Methacrylic acid	AIBN	Toluene	Ethylene glycol dimethacrylate	[80]	Ethanol

Caffeine	Methacrylic acid	AIBN	Acetonitrile	Ethylene glycol dimethacrylate	[81]	Soxhlet, Methanol: acetic acid (9:1)
Pentamidine	Methacrylic acid	AIBN	2-propanol: water	Ethylene glycol dimethacrylate	[82]	N/A
Theophylline	Methacrylic acid		Chloroform	Ethylene glycol dimethacrylate	[83]	Soxhlet, Methanol: acetic acid (9:1)
Verapamil	Methacrylic acid	AIBN	Chloroform	Ethylene glycol dimethacrylate	[84]	Soxhlet, Methanol: acetic acid (9:1)
Propranolol	Methacrylic acid	AIBN	Toluene	Ethylene glycol dimethacrylate	[85]	N/A
Naproxen	4-VP	AIBN	Toluene	Ethylene glycol dimethacrylate	[86]	Acetonitrile
Fluoroquinolones (Ciprofloxacin)	Methacrylic acid	AIBN	Dichloromethane	Ethylene glycol dimethacrylate	[87]	Acetonitrile: 4% formic acid (1:4)
Quercitin (Acrylamide)	TRIM	AIBN	THF	Ethylene glycol dimethacrylate	[88]	5 step Methanol mixtures

Atrazine	Methacrylic acid	AIBN	Chloroform	Ethylene glycol dimethacrylate	[89]	N/A
Cephalexin	TFMAA	AIBN	Acetonitrile	Ethylene glycol dimethacrylate	[90]	Methanol, trifluoroacetic acid
Bupivacaine	Methacrylic acid		Toluene	Ethylene glycol dimethacrylate and HEMA	[91]	N/A
Diazepam	Methacrylic acid	AIBN	Chloroform	Ethylene glycol dimethacrylate	[92]	Methanol, acetic acid (9:1)
Ciprofloxacin	Methacrylic acid	AIBN	Methanol: water (10:3)	TRIM	[93]	Methanol: acetic acid: trifluoroacetic acid (80:19.5:0.05)
Alfuzosin	Methacrylic acid	AIBN	Dichloromethane	Ethylene glycol dimethacrylate	[94]	0.5mL methanol + 1.5mL methanol: acetic acid (95:5)

Amoxicilin	Methacrylic acid	AIBN	Acetonitrile	Ethylene glycol dimethacrylate	[95]	N/A
Carbamazepine	Methacrylic acid	AIBN	Acetonitrile: toluene (75:25)	DVB	[96]	Soxhlet methanol
Zidovudin	Methacrylic acid	AIBN	Acetonitrile	Ethylene glycol dimethacrylate	[97]	Methanol: acetic acid (95:5)
Metronidazole	Methacrylic acid	AIBN	Dimethylformamide	Ethylene glycol dimethacrylate	[98]	Soxhlet, Methanol: acetic acid (9:1)
Ephedrine	Methacrylic acid	AIBN	Chloroform	Ethylene glycol dimethacrylate	[99]	Methanol: acetic acid (9:1)

2.5 Conclusions, challenges, and future developments

Since drinking water is a precious resource, it is imperative to maintain excellent water quality for the sake of safeguarding human health. Organic compounds such as MIB and geosmin can present unpleasant odors and numerous health risks, it is crucial to detect them in the early stage as this can prevent the health of organisms from serious threat. However, due to the low human OTCs as well as the complexity of raw water matrices, quantitative analyses on MIB and geosmin remain a significant challenge. A detection method required to be sensitive, selective, and reliable for trace screening of odorants at low concentrations (e.g., ppt), since many of these substances can be detected by olfactory senses (e.g., human noses) at ng/L levels. For establishing safety guidelines to those odorants and ensuring the security of drinking water for individuals, international authorities such as WHO have made tremendous contribution. Chromatography-based analytical methods such as GC-MS and HPLC-MS are the initial interest of scientific groups to identify odorous compounds in water due to their superior sensitivity, selectivity, and precisely quantitative capabilities. Up to present, this type of technique is still being widely used to make or update official guideline values or regulations to protect the public from potential taste and odor issues caused by MIB and geosmin. Nevertheless, labor intensive, time-consuming preconcentration steps are often required in these conventionally analytical methods, which involve large quantities of organic reagents or solvents, some of which are expensive, nasty, and environmentally harmful. This promotes the focus on developing a more effective detection platform capable of providing ultrasensitive results without hazardous reagents. Some alternates also show great promise including the bromine detection, chemiluminescence reaction, ELISA, and the BMD approach. However, most of them need to be conducted in scientific laboratories, in combination with professional characterization equipment to achieve the detection. Future demand looks towards cheaper and facile devices that can be transported for on-site detection. Electrochemical sensors and electronic tongues or noses provide potential avenues for rapid monitoring of MIB and geosmin without extensive clean-up procedures and expensive laboratorial equipment, offering a reliable and cost-effective solution for water quality assessment, public health safeguarding while maintaining the integrity of aquatic ecosystems.

The main challenge faced by drinking water utilities in their detection or removal is that pollutants contained can be determined at extremely low concentrations, down to ng/L (ppt) or even lower. Although there are a few breakthroughs after advent of electrochemical or electronic sensors, the creation of more advanced electrochemical measuring systems for ultrasensitive detection of MIB and geosmin in water sources are still subjected to several challenges [100, 101]:

- (1) High detection limits: the LODs of MIB and geosmin detected using electrochemical sensors or electronic devices (i.e., tongues or noses) are not as lower as those provided by chromatography-based methods such as GC-MS, with some of the LODs even higher than values obtained from conventionally analytical methods in a couple of orders of magnitude, according to literatures reviewed.
- (2) Interfering from other organic or inorganic compounds in water: there are different organic or inorganic substances may interfere with MIB and geosmin detection under an electrochemical measurement, therefore of causing erroneous readings in analysis of water samples. It is extremely difficult to create sensors that possesses high selectivity for MIB and geosmin with little interference from other compounds. MIPs are often used in sensor fabrication however they can only provide structural resistance against organic chemicals or biomolecules but not ions or other inorganic components.
- (3) Sensor fouling and poor stability: electrochemical or electronic sensors may be subjected to fouling problems due to the accumulation of pollutants or biofilms on the electrode surface over time. It is highly crucial to ensure long-term stability and reliability of the sensor response especially for applications involving continuous monitoring.
- (4) Lack of effective sensor calibration: given changes in sensor responses over time and between various water sources, it may be difficult to calibrate sensors to achieve precisely measurements on concentrations of MIB and geosmin, therefore of great importance in creating standardized calibration procedures for this type of sensors.

Specifically, future development upon traditionally analytical methods (i.e., chromatography-based methods) can involve automation of preconcentration steps, which is preferential for routine commercial applications where large volume of sample batches are daily analyzed. Additionally, faster extraction or microextraction techniques with smaller sample requirements will significantly improve both analysis timeframes and costs. For future on-site use of electrochemical or electronic sensors, it is concerned that the sample analysis needs to be as clean as possible because many of detection sites are sources of drinking water. The sensing method without adverse effects on the quality of drinking water will be applied as a priority. More importantly, the idea for electrochemical and electronic sensors would be, due to their lifespan being unique compares to any other detection method, installing the devices inside pipelines which feedback to a system or be incorporated into the distribution networks of water utilities to allow for automated and continual network monitoring in different places, providing a bright future for real-time and long-term detection.

In fact, the cost effects of current detection methods are still not applicable to a large-scale sample analysis. Based on the discussions, an ideal method of detection upon odour compounds are yet to be, or to some extent, not to be fully established. Future designs for detection systems are desirable to be focused on following natures including: (1) simple and compact devices; (2) less time consuming in data analysis; (3) higher sensitivity and accuracy in the range of ng/L or below; (4) less labour in device fabrication or experimental operation; (4) capability of on-site monitoring; (5) no or less impact on the natural environment; (6) cost-effectiveness with technical feasibility; (7) easy to perform calibration; (8) without sample destructive steps or not be regarded as a sample destructive method; (9) any part of the method are not restricted to one-time use (excellent component availability or reproducibility); (10) instrument reusing in completing analyses for a different sample. In any case, there remains a strong desire for new analytical innovations to enable more sensitive, simpler, and faster detection methods to be performed on-site with close to real-time determination. A multidisciplinary strategy incorporating knowledge of materials science, electrochemistry, sensor technology, water quality monitoring, and

environmental engineering is necessary to meet these issues to make future assembles for MIB detection more efficient and dependable, providing better water quality monitoring as well as protection for health of the public.

Chapter 3 Theoretical Background

3.1 Electrochemical Properties

3.1.1 Redox Reactions and Electrode Potentials

A redox reaction simply describes a state of reaction where one species loses electrons, and therefore is oxidised, and another gains electrons, and therefore is reduced in overall charge. This encumbers an incredibly wide range of reactions, dating back as far as 6000BCE with the heating of copper ore to form copper metal with coal, where the ore is reduced, and the coal is oxidised to form carbon dioxide [102].

There are 5 primary types of redox reactions, combinations, decompositions, displacements, combustions and disproportionations. Combination describes two elements combining, one becoming oxidant and the other reluctant; decomposition describes a compound being broken down into its individual elements; displacement describes one or more atoms being swapped out for another; combustion describes a compound reacting with oxygen to produce carbon dioxide, water and heat; while disproportionation describes a molecule being both reduced and oxidised [102]. In electrochemistry, the potential difference between the working electrode and the reference electrode is critical in driving the reactions themselves.

The electrode potential is the measurement of the tendency of a chemical species to gain or lose electrons, this can be described quantitatively through the Nernst equation, which allows for the calculation of the electrode potential [103]:

$$E = E^0 + \frac{RT}{nF} \ln \frac{|Ox|}{|Red|} \quad (1)$$

Where E is the electrode potential, E^0 is the standard electrode potential for the redox reaction, R is the universal gas constant, T is the temperature in kelvin, n is the number of electrons transferred in the reaction, and F is the Faraday constant. While the right fraction is the concentration in oxidised form over the concentration in reduced form.

3.1.2 Types of Electrochemical Sensors

The types of electrochemical sensors are classified into categories based on the type of electrical signal they measure. These categories are as follows:

- Amperometric Sensors: Which measure the current resulting from the redox reaction at a constant potential. These are highly sensitive and provide quantitative data on the concentration of the analyte. These are used widely in detecting glucose in blood, environmental pollutants, and biological molecules [103].
- Potentiometric sensors: Measure the potential difference between the working and reference electrode without drawing any current. These are advantageous for their simplicity and low power requirements, while being used commonly in pH meters and ion-selective electrodes [104].
- Impedimetric sensors: These measure the change in the electrical impedance of the sensor, which can then be correlated with the analyte concentration. These sensors are useful for detecting binding events at the sensor surface, making them viable for biosensing applications, such as the use of an MIP [105].

3.2 Analytical Techniques for Sensor Characterisation

3.2.1 Cyclic Voltammetry

Voltammetry describes the technique of current measurement during variation in the potential between two electrodes, where a current is produced through the electron transfer between the redox species and the two electrodes. Cyclic voltammetry (CV) is one of many voltammetry techniques, described as a potential sweep method where an electrode is submerged in an unstirred solution with a cycling potential, where the resulting current is measured. CV is performed using a three-electrode system, consisting of the working, reference and counter electrode. The measured potential of the working electrode is controlled versus the reference electrode, typically being either a saturated calomel electrode, or a silver/ silver chloride electrode.

This form of analysis allows for a basic understanding of the electrochemical profile, providing information on the base characteristics of the working electrode. CV has been used widely as a preliminary analysis technique for characterization prior to further testing due to the low cost, simplicity and speed of testing, as well as a lack of in-depth training required to carry out.

CV provides data in the form of a Voltammogram or Cyclic voltammogram, where the x-axis is represented by the potential in voltage passing through the electrode, while the y-axis is represented by the measured current in Amps. An understanding of the Nernst equation (equation 1) allows for the characteristic shape of the Voltammogram to be understood, along with the peaks associated with them.

3.2.2 Electrochemical Impedance Spectroscopy

Electrochemical Impedance Spectroscopy (EIS) is a powerful and non-destructive analytical technique used to investigate the interfacial properties of electrode systems. EIS allows for the study of the electrical properties of the electrode-electrolyte interface by applying a small AC voltage and measuring the resulting current response over a range of frequencies. This technique allows for an insight into charge transfer processes, surface modifications and analyte interactions when used alongside an electrochemical biosensor.

EIS measures the frequency-dependent impedance (Z) of an electrochemical system, typically represented in the Nyquist plot (real against imaginary impedance) or a bode plot (impedance magnitude and phase shift against frequency). The impedance response is influenced by various interfacial components such as:

- Solution resistance (R_s): Represents the resistance of the bulk electrolyte solution between the working and reference electrodes. It reflects the ionic conductivity of the medium and is typically observed as the high-frequency intercept on a Nyquist plot. A higher R_s indicates a lower ionic strength or poor conductivity in the electrolyte.
- Charge transfer resistance (R_{ct}): Corresponds to the resistance faced by electrons during redox reactions at the electrode surface. It is strongly influenced by the electrode material, surface modification (such as MIP

layers), and the presence of the analyte. An increase in R_{ct} often signifies hindered electron transfer due to analyte binding or insulating film formation.

- Double layer capacitance (C_{dl}): Represents the capacitance formed at the electrode-electrolyte interface due to the separation of charges. Physically, it arises from the accumulation of ions at the electrode surface, forming the electrical double layer. C_{dl} is affected by the electrode surface area, roughness, and dielectric properties of the interface. In biosensors, variations in C_{dl} indicate changes in surface coverage or analyte interactions.
- Warburg impedance (Z_w): Models the diffusion of electroactive species to and from the electrode surface. It manifests as a straight line with a slope of 45 degrees in the Nyquist plot at low frequencies. Physically, it represents the time-dependent mass transport limitations of ions in solution. This component becomes significant when diffusion is the rate-limiting step in the sensor response.
- Constant Phase Element (CPE): Used in place of an ideal capacitor to account for non-ideal interfacial behaviour. The CPE models distributed capacitance caused by surface roughness, heterogeneous film coverage (such as MIPs), or varying local dielectric properties. Mathematically, it introduces a phase angle that deviates from 90°, characteristic of an ideal capacitor. The CPE is especially applicable in real biosensors where uniform surface conditions are difficult to achieve.



Figure 6: Electrochemical impedance spectroscopy equipment used throughout testing

3.3 Material Characterisation

3.3.1 Scanning Electron Microscopy (SEM)

SEM is an analysis method which allows for the examination and analysis of micro- and nanoparticle imaging of solid objects through the use of electron emission, providing grey-scale images of magnification up to 300,000x. SEM is the most expensive and detailed form of microscopy, being compared to optical microscopy which has a magnification range of 400-1000x and showing images in their true colours. A Scanning Electron Microscope consists of several components [106]:

- A source to generate electrons of high energy.
A column down for the travel of electrons through two or more electromagnetic lenses.
- A deflection system consisting of scan coils.
- An electron detector for backscattered and secondary electrons.
- A sample chamber.

A computer system consisting of viewing screens to display the scanned images and keyboard to control the electron beam.

3.3.2 Raman Spectroscopy

Raman Spectroscopy is a scattering technique based on the Raman effect, stating that a frequency of a small fraction of scattered radiation is different from frequency of monochromatic incident radiation. This technique is based on the inelastic scattering of incident radiation through the interaction with vibrating molecules, probing the molecular vibrations [107].

In Raman Spectroscopy, the sample surface is illuminated with a monochromatic laser beam which scatters in all directions, developing a scattering of light. A large percentage of the scattered light is at a frequency equal to that of incident radiation, constituting as Rayleigh scattering, however, the remaining has a frequency which differs from incident radiation. This differing frequency radiation allows for the construction of a Raman spectrum due to inelastic collisions between incident monochromatic radiation and surface molecules of the sample.

3.3.3 BET nitrogen adsorption analysis

BET or Brunner-Emmett-Teller nitrogen adsorption analysis is a technique used to identify the specific surface area of a sample to the atomic level through the utilisation of an inert gas (N_2 in this case). This is achievable through the maintenance of the temperature on the sample surface alongside the increase in pressure of the inert gas applied. The formation of gas molecules on the surface of the sample forms a layer encompassing the entirety of the surface. This allows for the adsorption of remaining nitrogen atoms not present in the formed surface layer to directly correspond to the number of nitrogen atoms either present in the layer, in pores on the surface or simply remaining nitrogen atoms around the surface. Due to the understanding of the cross-sectional surface area of nitrogen atoms, and an understanding of the relationship between gas adsorption as a function of pressure, the accessible surface area of the sample can be calculated from the BET equation:

$$\frac{P}{v(P_0 - P)} = \frac{1}{v_m C} + \frac{C - 1}{v_m C} \left(\frac{P}{P_0} \right) \quad (2)$$

The BET equation allows for the calculation of the volume of nitrogen adsorbed (v) at the applied pressure (P), using the volume adsorbed in one complete unimolecular layer (v_m), the appropriate constant (C) and the base pressure of the system (P_0) [108].

3.4 Principles of Molecular Imprinting Method

The theory of molecularly imprinting aims to mimic the functionality of an antibody, without the use of organic material. This works through the creation of binding sites on a polymer surface through the introduction, removal, and re-introduction of a target molecule. The initial introduction of the target molecule takes place during the creation of the polymer, where the target molecule, functional monomer, initiator, solvent and cross linker are mixed under required conditions depending on the chosen compounds. This mixture is then placed in the correct conditions based on the initiator compound for the polymerization process to take place. Following the synthesis of the polymer, a solvent or solution is introduced to the surface to encourage the removal of the target molecule from the polymer, creating a polymer matrix. This polymer matrix contains binding sites specific to the structure of the target molecule. These binding sites then encourage the re-binding of the target molecule during reintroduction. The rebinding of the target molecule allows for the

sensitive detection of its presence in a provided sample based on the comparison to previously tested controlled concentrations.

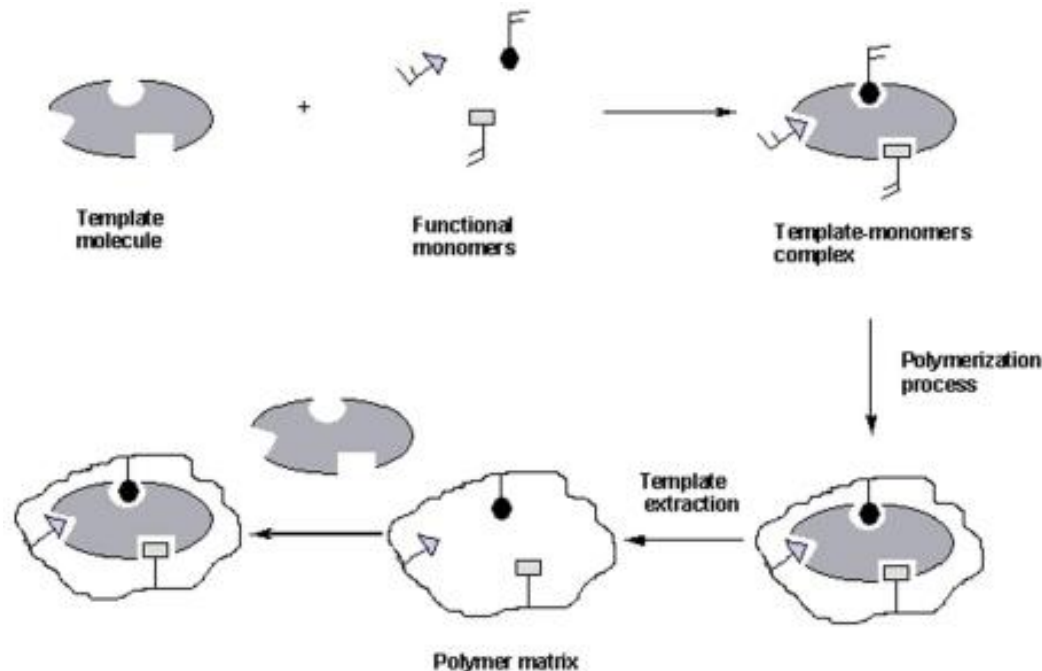


Figure 7: Scheme of Molecular Imprinting [109]

4Materials and Methodology

4.1 Chemicals and Reagents

The Graphene, MIB, Ethylene Glycol Dimethacrylate (EGDMA), Hexane, Azobisisobutyronitrile (AIBN), Potassium Ferricyanide, Phosphate Buffered Saline (PBS) and Methacrylic Acid (MAA) were all purchased from Sigma Aldrich, while the Diacetone Alcohol (DAA) was purchased from MP Biomedicals, the E15/48A was purchased from Wacker Chemicals Limited and Methanol was purchased through Thermo Fisher Scientific. Deionised water was used throughout the experiments.

4.2 Electrochemical Sensor Fabrication via Flexographic Printing

To begin, 4g graphene and 40g DAA were mixed in a ball mill for 16-20 hours at 250rpm to prepare the carbon ink. After this initial mixing, 45mL of 0.2mg polydopamine (PDA) solution was added to the pot and mixed for a continued 30-60 minutes, again at 250RPM. Following this, 3g of E15/48A and 50g DAA were added, and the resulting mixture was mixed for 10 hours at 250rpm. The mixture was initially test printed onto white PVC sheets to assess the structure of the ink, then moving to a Kapton polyimide tape for the final product. All printing was carried out at room temperature (25°C). Each print was carried out through 6 rotations of the plates, with a blow gun set to 200°C being used to dry the ink attached to the sheet between each rotation. Following this process, the sensor sheet is then placed onto a

hot plate at 80°C for 10 minutes to allow of the ink to sufficiently set. Once the ink is set, the sensors are placed into an oven at 300°C for 30 minutes.

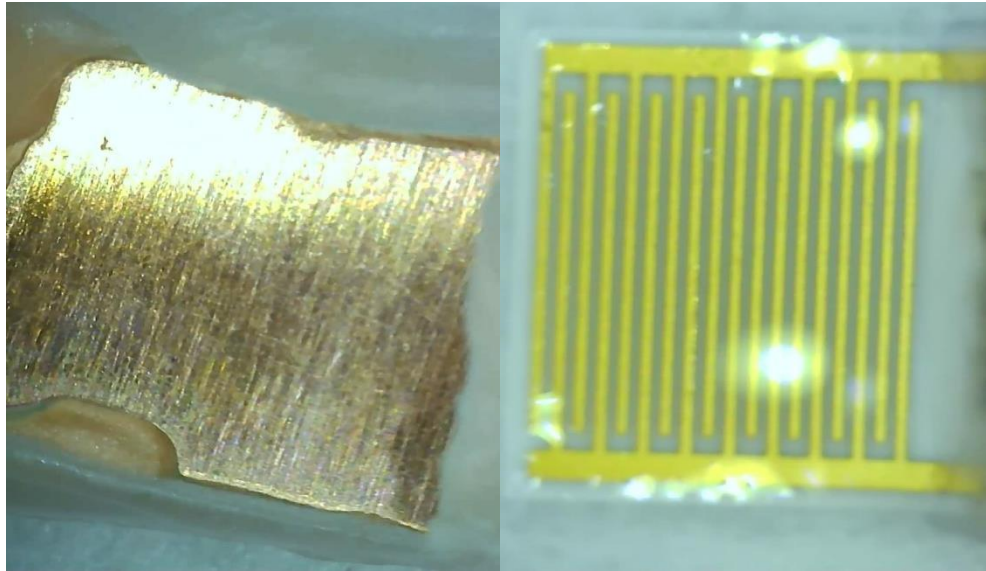


Figure 8: The copper strip surface (left) and gold electrode surface (right) through a microscope

4.3 Preparation of the MIPs

4.3.1 Compound Selection for the Polymer The selection process for the compounds used in the polymer mixture can be a rigorous process due to identifying the most efficient for the target molecule. To identify the ideal polymer recipe, an in-depth review on current compound choices was carried out and the target molecule compared to that of 2-MIB. The selection of the initiator, cross-linker and functional monomer are consistent across the majority of MIPs in literature, being AIBN, Ethylene glycol dimethacrylate and methacrylic acid respectively. The solvent used throughout the testing was decided based on previous MIB research, as well as initial testing with the chose solvent proving positive, this being hexane.

4.3.2 Polymerization Process and Conditions

The polymerization process begins with the preparation of the sensors, isolating the interdigitated surface area through the use of an epoxy mixture. A mixture of 25 μ L hexane, 2.6mg MIB, 8.5 μ L MAA and 25 μ L EGDMA is initially created to begin the polymer production. This is first mixed for around 2 minutes at 700RPM. Once

completed, 1.1002mg AIBN is introduced to begin the polymerization, which is now mixed for a further 10 minutes. The resulting solution is now pipetted onto the isolated, interdigitated surface of the sensors using a drop casting method, which are then left at 40°C for 48 hours to complete the process.

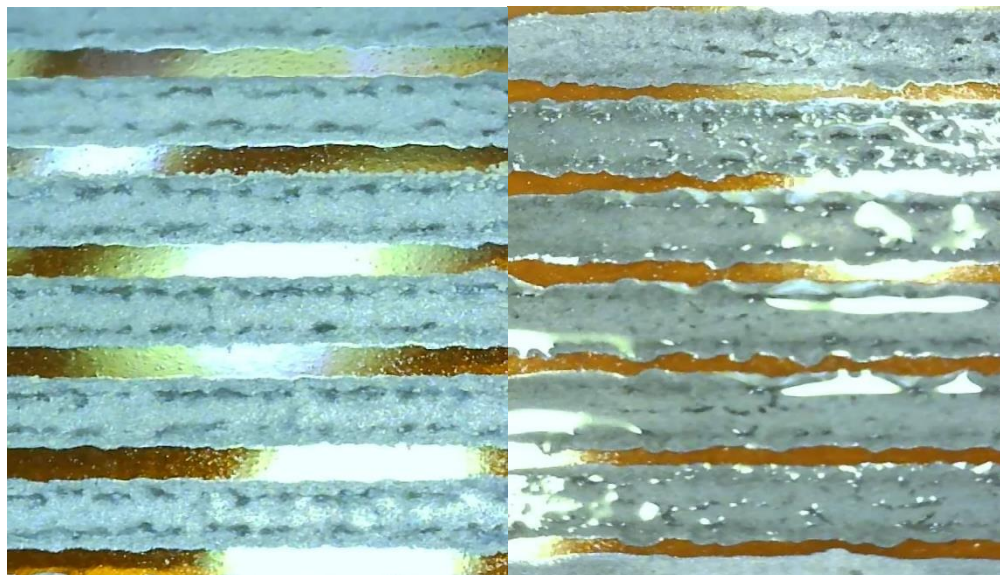


Figure 9: The carbon electrode surface before (left) and after (right) MIP application.

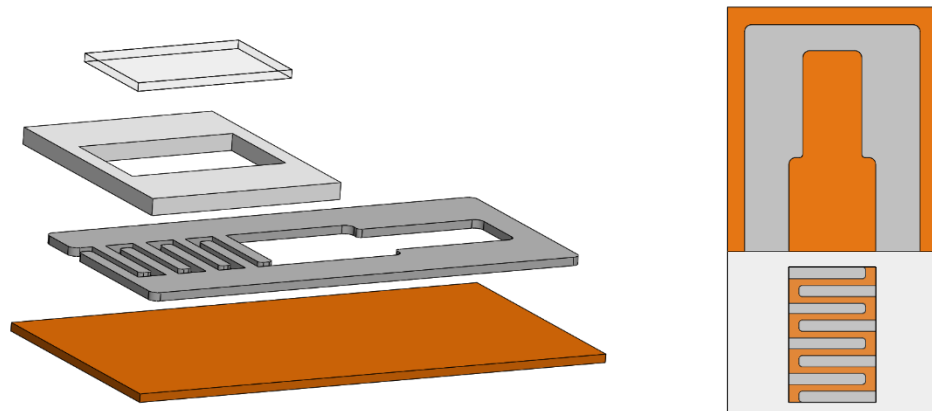


Figure 10: Explosive (left) and top-down (right) view of an example carbon electrode, showing the MIP, epoxy, carbon and polyimide layers.

4.3.3 Template Molecules Removal

The NIP or MIP sensors were placed into a container holding a volume of liquid which sufficiently submerged the interdigitated section of the sensor. A clamp stand was placed to allow for the container to be placed into the water of an ultrasonic bath sufficiently, so the liquid contained was entirely submerged. Throughout the

research, the liquids used consisted of ethanol and methanol at varying concentrations, mixed with deionised water. Ultrasonication was carried out for a duration of 25 minutes. Once the sensor was removed from the container, it was rinsed with deionised water, ensuring the pressure is applied not onto the interdigitated surface, but is allowed to run across it. This allows for the removal of any solution still on the sensor surface.



Figure 11: Overall (Left) and enlarged (Right) template removal technique with beaker, sensor, removal solution and stirrer.

4.4 Cyclic Voltammetry Testing

Cyclic voltammetry testing was carried out using an octostat (Octostat30, Ivium), a silver / silver chloride reference electrode, and a gold counter electrode in a 3-electrode circuit. To begin, a clamp stand was positioned to ensure all 3 electrodes could be placed into a beaker containing an electrolyte solution consisting of potassium ferricyanide. The sensor to be tested was then placed into the stand, submerged into the electrolyte solution sufficiently, to submerge the interdigitated section of the sensor, also ensuring that the other 2 electrodes are submerged. All CV testing used the settings as follows: E start 0V, Vertex 1 0.8V, Vertex 2 0V, E step 10mV, N scans 10cls, Scanrate 100mV/s, Equilibration time 30s, Current range 10mA, 4-electrode system, Max range 100A, Min range 100nA.

4.5 Electrochemical Impedance Spectroscopy

Electrochemical Impedance Spectroscopy was carried out through the use of an octostat in a 2-electrode system. The sensor was connected to the octostat and

stability was ensured through the use of tape on the clips and cables themselves. 100 μ L of the electrolyte solution of potassium ferricyanide was then deposited onto the interdigitated surface of the sensor using a drop casting method. All EIS testing used the settings as follows: E start 0V, Equilibration time 0s, 40 frequencies from 1000HZ to 0.05Hz, Current range 10mA, 2-electrode system, Max range 10mA, Min range 10nA, Monitor time 120s, Monitor interval 1s.

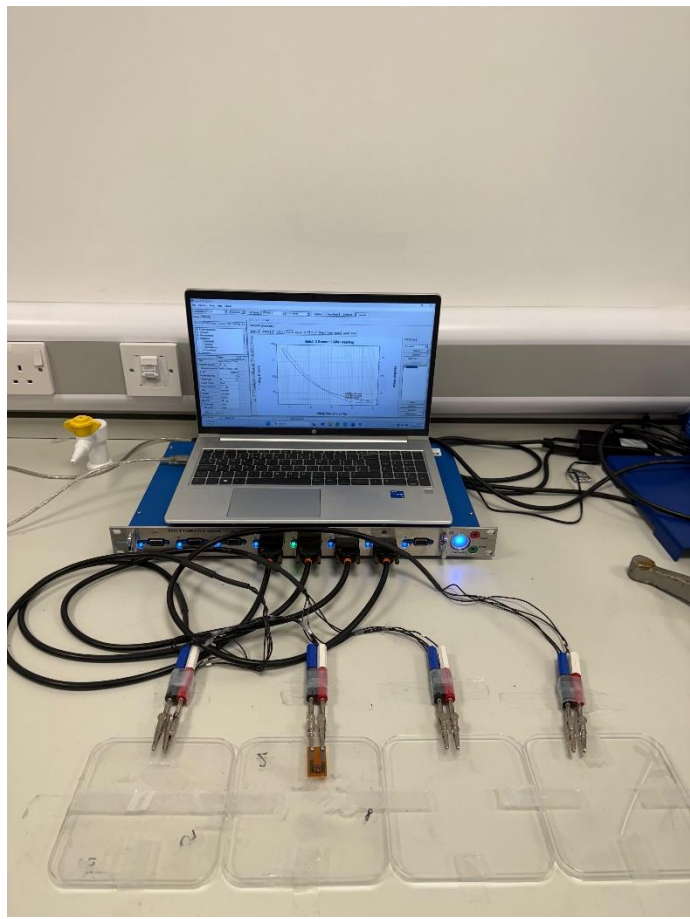


Figure 12: EIS testing setup with multiple outputs, using the OCTOSTAT, showing the 2-electrode setup used throughout testing

5Results and Discussion

5.1 Electrochemical MIP Sensor Preparation and Optimization

In this study, the optimisation to the key parameters of the sensor were seen as the most important aspect, such as the volume of polymer applied to the sensor and the required oven polymerisation time. The volume of polymer applied to the sensor is important in determining the efficiency on the sensor underneath, as well as the sensitivity of the polymer itself. To determine this, sensors were taken before and after polymer application to assess the change in current, as well as comparing the CV results between a range of different volumes.

To begin, the electrode composition was considered and tested to assess the effect of the carbon electrode against that of gold or copper, CV tests were carried out as seen in figure 10 to assess this, leading to the prolonged use of carbon.

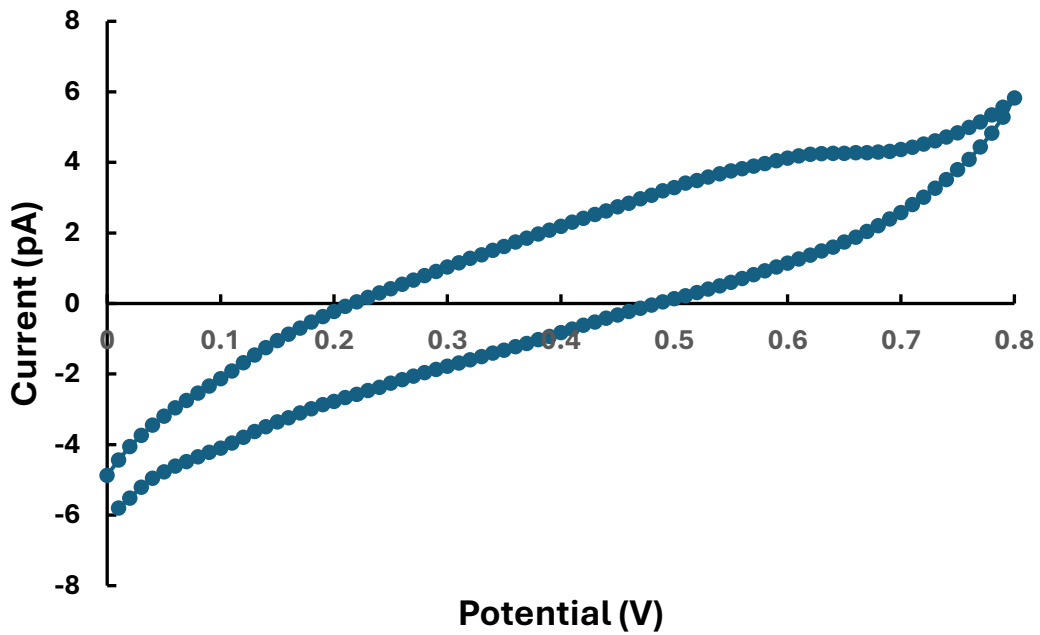


Figure 13: Cyclic voltammetry results from a clean gold electrode

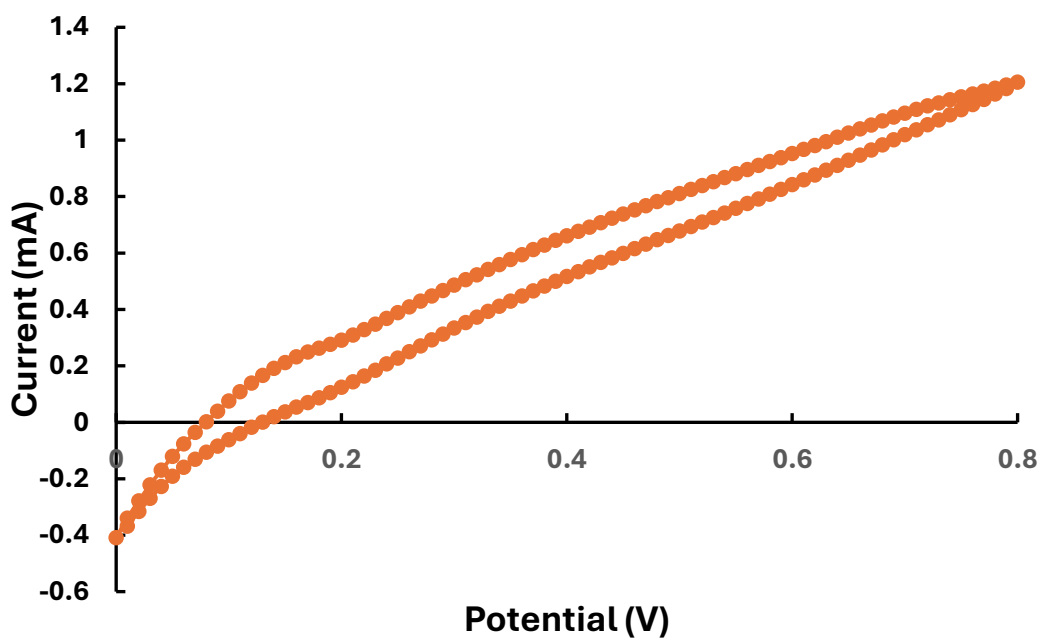


Figure 14: Cyclic voltammetry results from a clean copper strip

Figures 13 and 14 show the non-ideal nature of both the copper and gold electrodes, with the current measurement from the gold electrode being produced in pA as opposed to the expected mA.

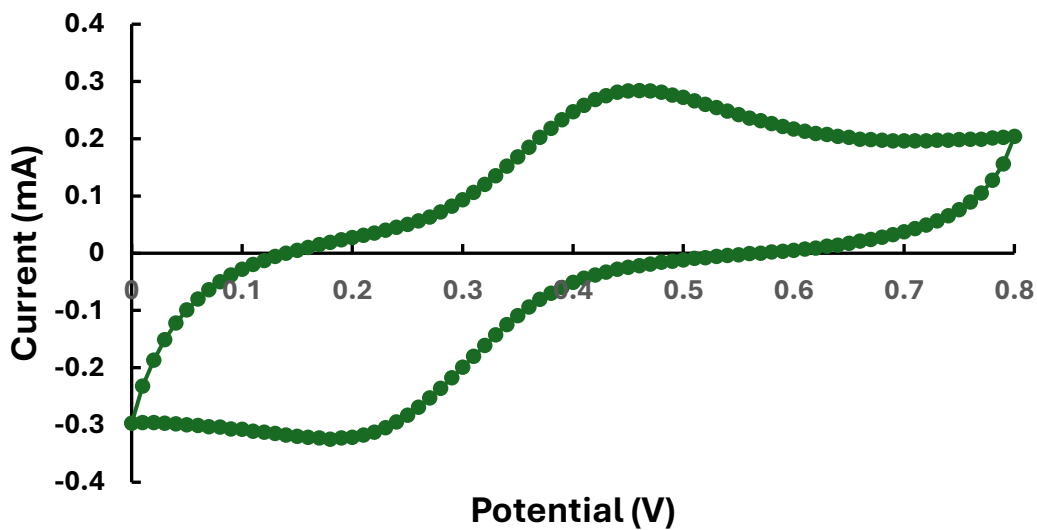


Figure 15: Cyclic voltammetry results from a carbon-based electrode following a 30-minute oven curing time

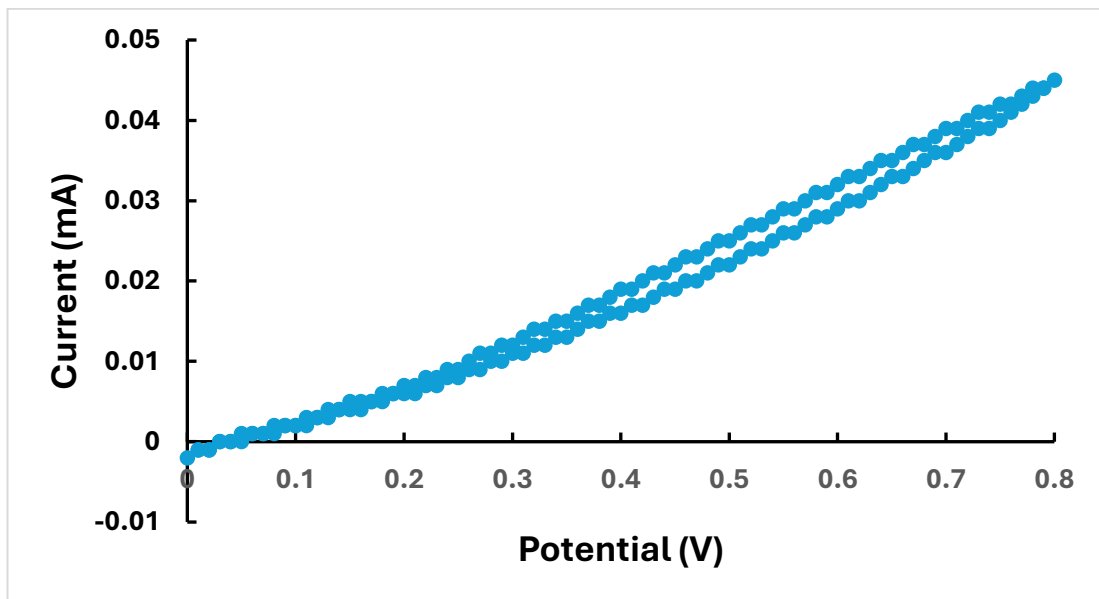


Figure 1615: Cyclic voltammetry results from a carbon-based electrode following a 15-minute oven curing time

The effect of the length of oven curing time was assessed following initial printing, with the CV test results shown in figures 15 and 16 being assessed, with 30-minutes used throughout further testing.

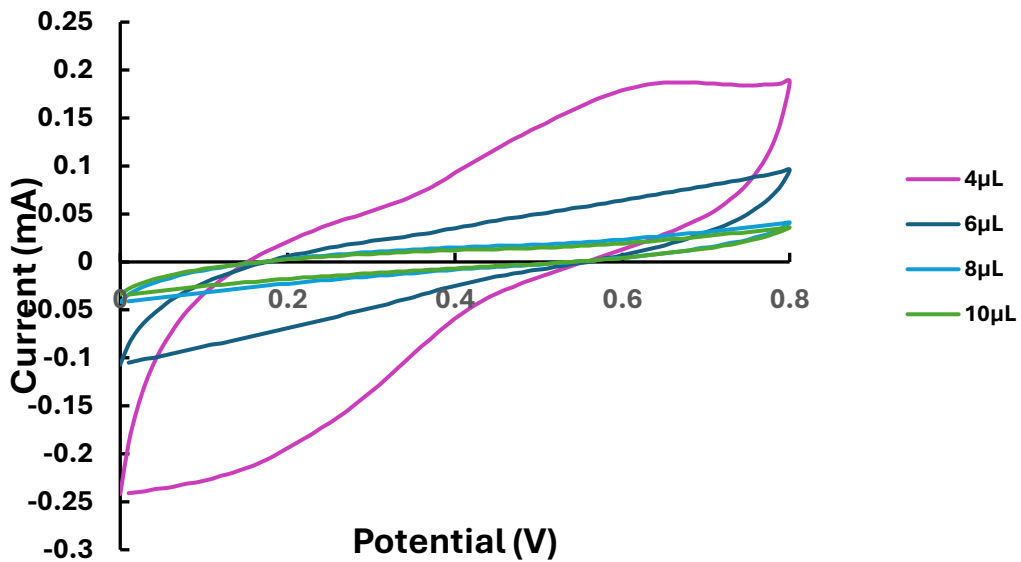
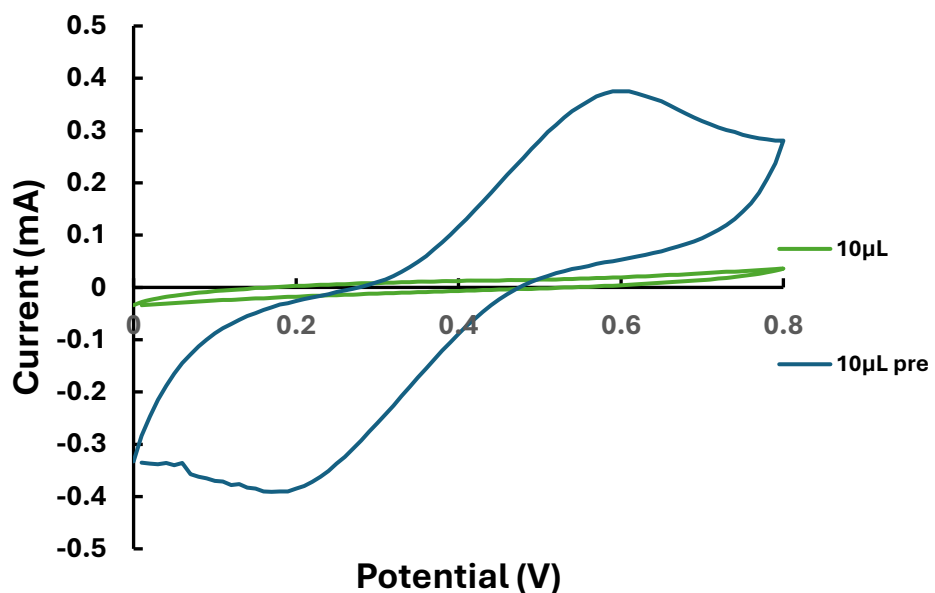


Figure 167: Cyclic voltammetry results from sensors post polymer application from 4 to 10 μL , in 2 μL increments

Figure 17 allowed the conclusion to be drawn that the change in current based on the increase in polymer volume is drastic until a polymer volume of 8-10 μL is applied to where a further increase has little to no effect. The change in peak current



between before and after polymer application was evident, as seen in figure 18, and was assessed through all volumes tested to identify the most efficient to move forwards with.

Figure 178: Cyclic voltammetry results from a sensor before and after the application of polymer.

5.2 Template Molecules Removal

The primary concern with identifying the solution to use during the removal of the template molecules is the effect it can have on the polymer layer itself. Due to the capability to erode the top layer of the polymer surface, removing the binding sites for the target molecule, the washing solution was tested against non-imprinted sensors. This would allow the effect of the solution on the base polymer later, without seeing the effects of the removal of the target molecules. To begin, a washing solution of 100% ethanol, and methanol and acetic acid in an 80:20 mixture, as shown in figures 19 and 20.

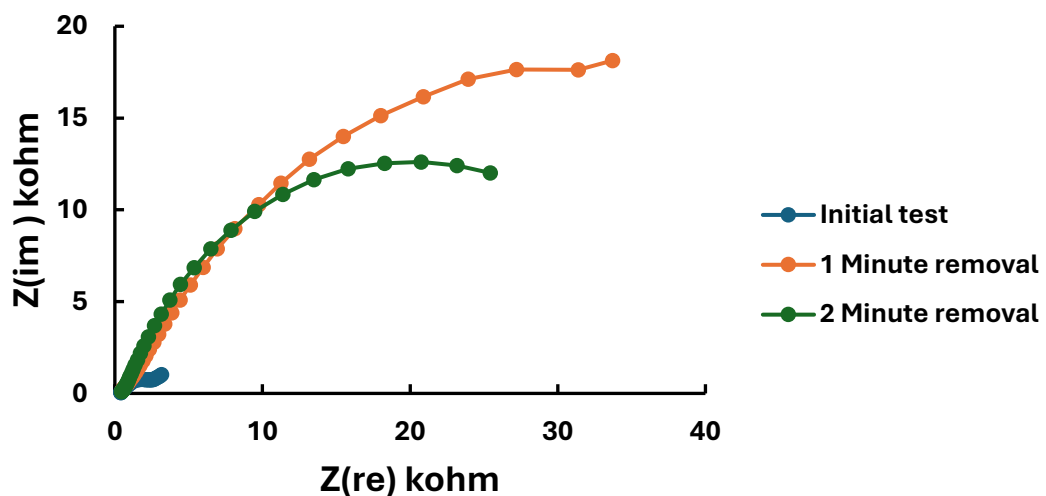


Figure 18: Nyquist plot results from a methanol and acetic acid mixture used as the washing solution for an initial test using NIP, 1-minute and 2-minute removal time.

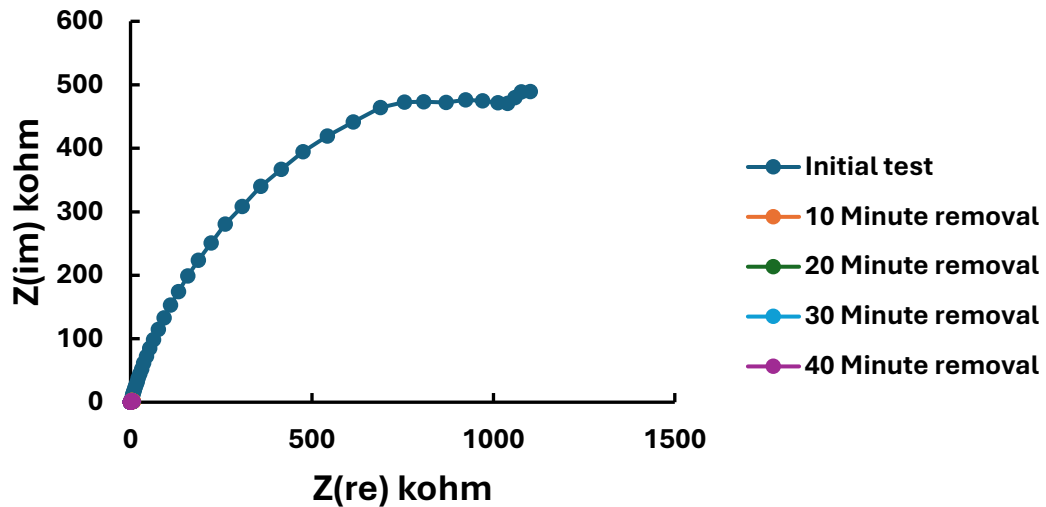


Figure 19: Nyquist plot results from a 100% ethanol solution used as the washing solution with an MIP layer for an initial test to 40-minute removal time using 10-minute increments.

Figures 21-23 allow for the observation that the use of template molecules in the polymer has little effect on the results using a 100% ethanol solution, as an initial drastic change can be seen, which is then reduced to minimal change following the initial 10-minute removal time.

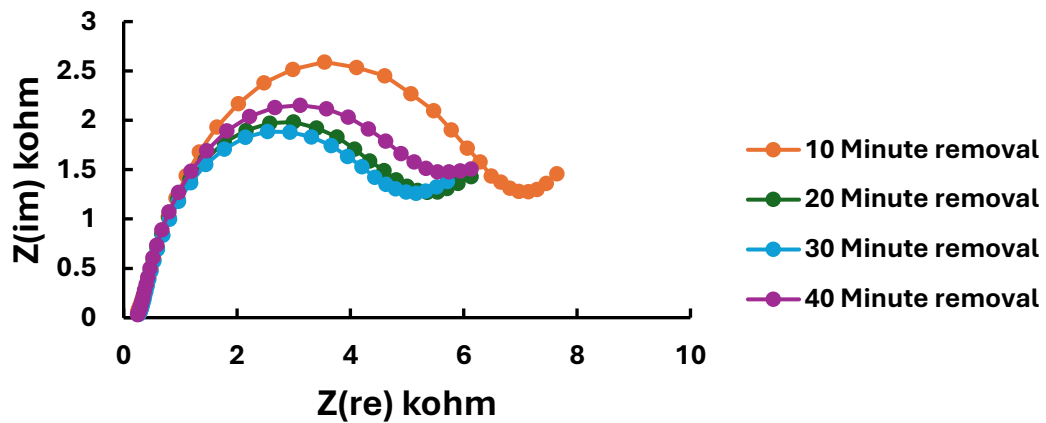
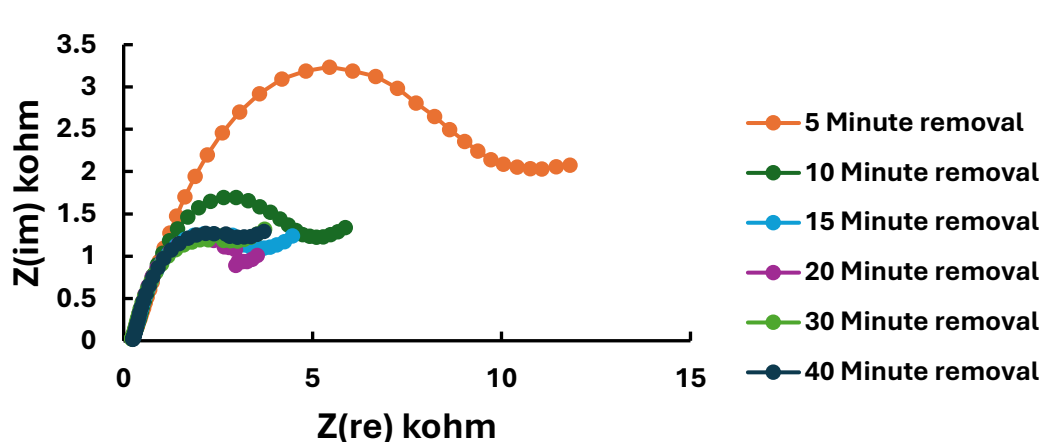
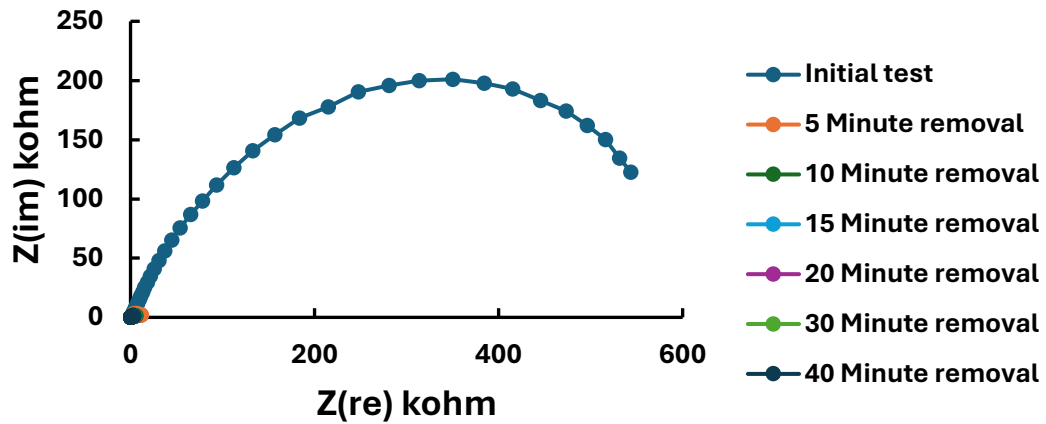


Figure 20: Nyquist plot results from a 100% ethanol solution used as the washing solution with an NIP layer for a 10-minute to 40-minute removal time using 10-minute increments.



Lower ethanol percentage solutions were then used alongside ultrasonication. As seen in figures 24 and 25, a maximum change of around 5% can be observed when using an NIP, with consistency shown similar to that of variation seen often between sensor testing.

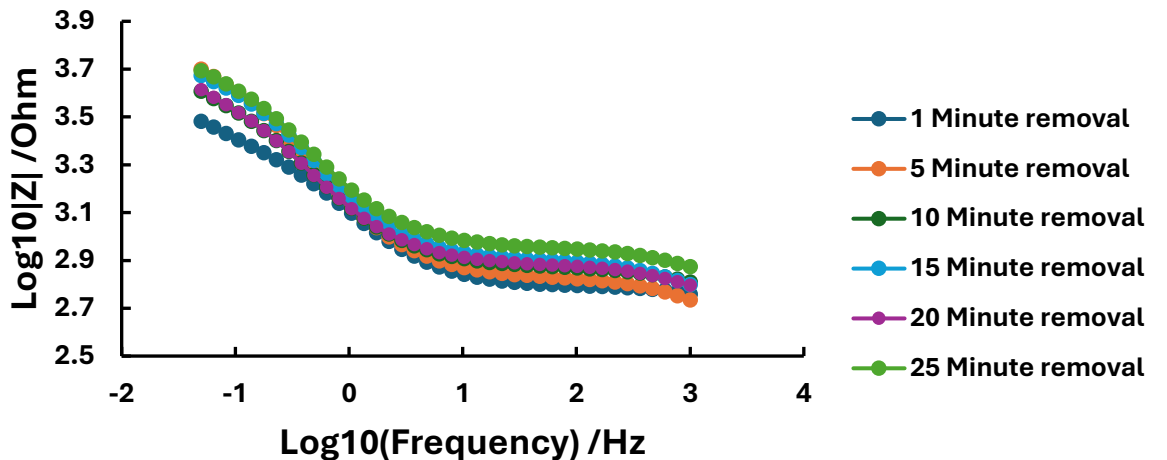


Figure 23: Bode plot from Electrochemical Impedance Spectroscopy of an NIP washed with 1% ethanol in an ultrasonic bath between 5 and 25 minutes, in 5 minutes intervals.

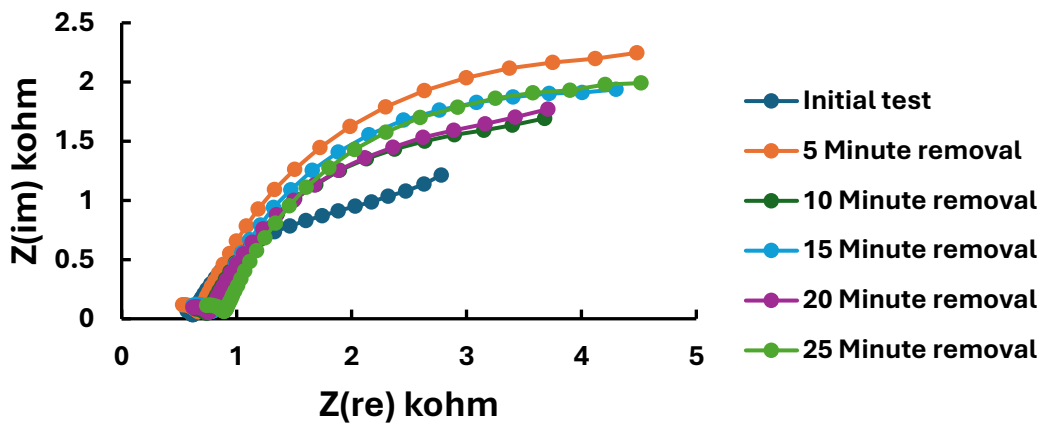


Figure 24: Nyquist plot from Electrochemical Impedance Spectroscopy of an NIP washed with 1% ethanol in an ultrasonic bath between 5 and 25 minutes, in 5 minutes intervals.

From the tests shown, a 25-minute removal time was chosen for use throughout testing due to the consistency shown in order to ensure thorough template removal, as the change leading up to and following 25 minutes can be seen as minimal for time consumption.

5.3 Reintroduction of the Target Molecules

The reintroduction of the target molecule is vital for the sensor's ability to react to the target molecule in a testing sample. Figure 23 shows the change in resistance from a prepared sensor, to being washed, and then to the reintroduction of the target molecule, with the trend returning after 1 hour of reintroduction to the state at which it began. Increasing the reintroduction time above 1 hour showed to allow for the continual increase of the resistance of the sensor, while still returning to a lower state following the removal process.

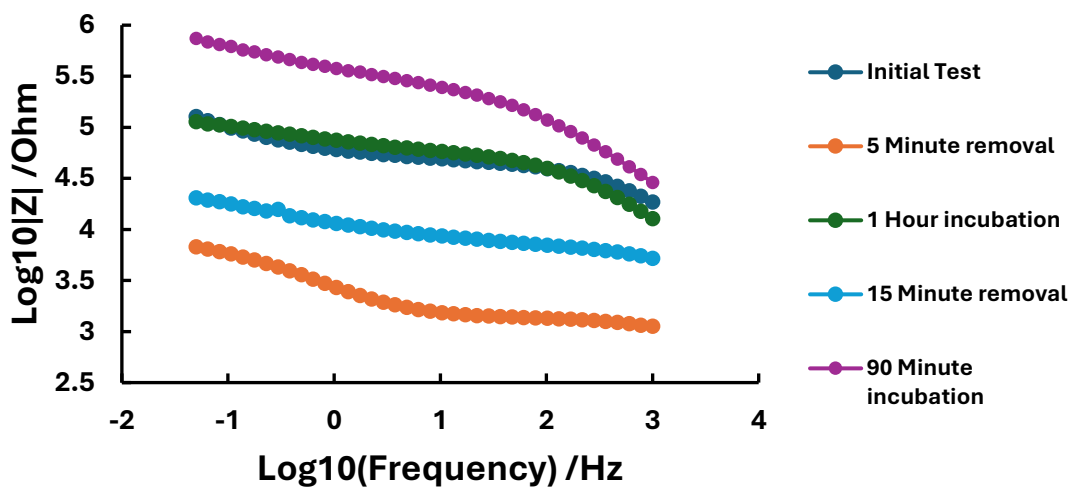


Figure 25: Bode plot from Electrochemical Impedance Spectroscopy of an MIP through stages of removal and reintroduction of the target molecule

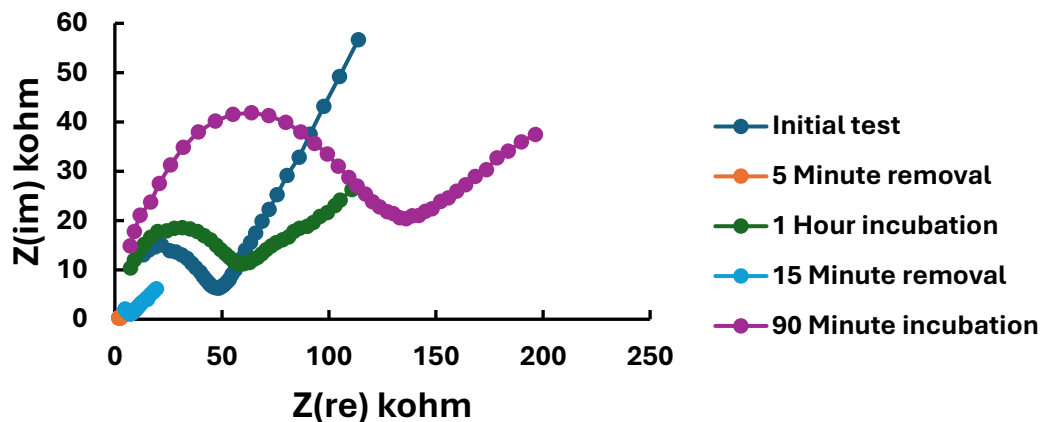


Figure 26: Nyquist plot from Electrochemical Impedance Spectroscopy of an MIP through stages of removal and reintroduction of the target molecule

Figure 26 also shows that the initial 5-minute removal of a sensor has more of an effect than subsequent washes following a reintroduction period, with the initial 5-minute wash causing a 25.5% decrease, and the subsequent 15 minute wash following reintroduction causing a 15.7% decrease.

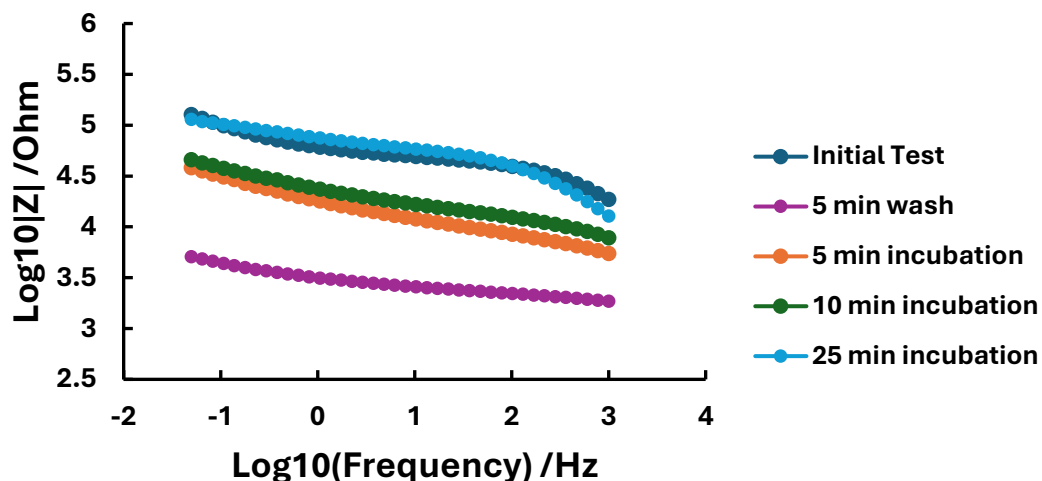


Figure 27: Bode plot from Electrochemical Impedance Spectroscopy of an MIP during reintroduction time optimization testing

To finalise reintroduction testing, an MIP was reintroduced to the target molecule with the aim of the electrochemical response returning to the state of the initial polymerization, as theoretically binding sites have been restored to the same state as before template removal. From figure 25, a reintroduction time of 25 minutes was identified as ideal.

5.4 MIP Sensor Characterization

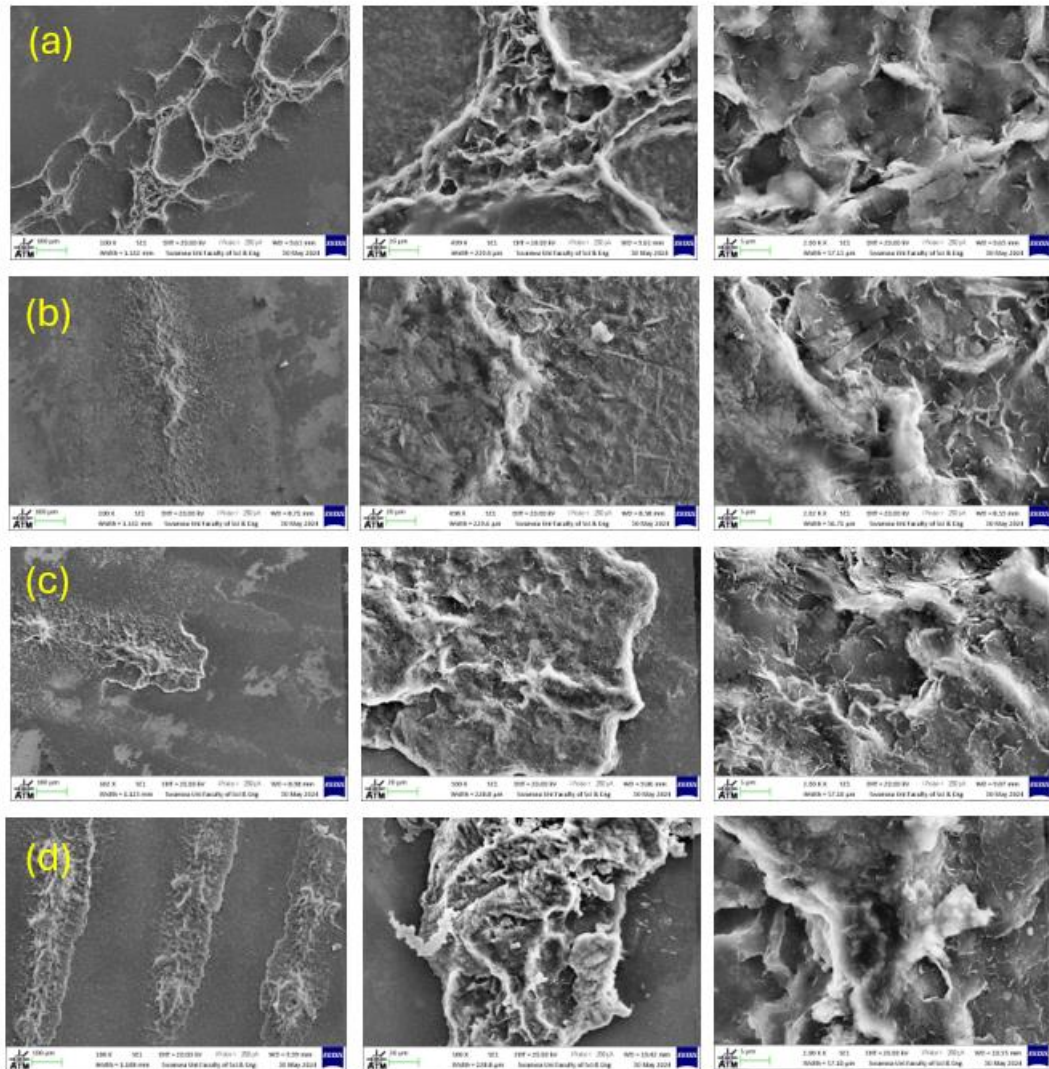


Figure 28: Electron micrographs showing the surface morphologies of the interdigitated surface of a sensor following (a) non-imprinted polymer application, (b) imprinted polymer application, (c) post template removal of an imprinter sensor and (d) post reintroduction of the target molecule. Columns increase in magnification from left to right, with fields of view of 100, 20 and 5 μ m.

Figure 26 shows SEM imaging of sensors through the stages of testing, non-imprinted polymer application, imprinted polymer application, template removal and template reintroduction respectively. As can be seen throughout the stages, the porous surface of the interdigitated graphene sections differs to the more uniform spaces between, with little differences following the presence of the target molecule.

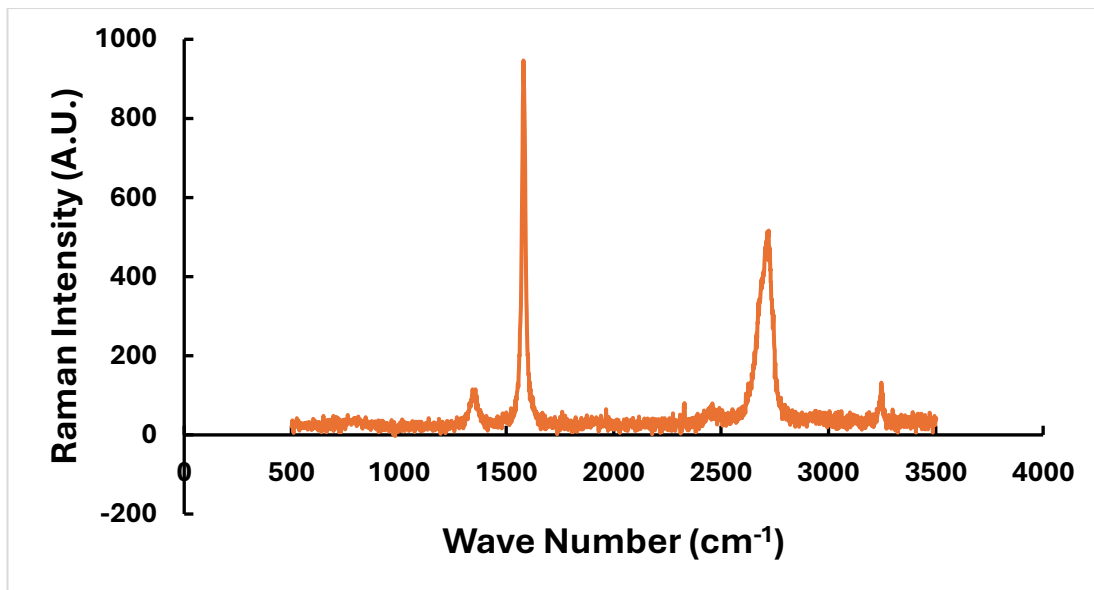


Figure 29: Raman spectroscopy data for the commercial graphene used in the fabrication of the sensor

Raman spectroscopy data was taken for the commercial graphene used for the sensors throughout testing. As seen in figure 27, the distinct G and 2D peaks are evident in the 1580cm^{-1} and 2710cm^{-1} regions, showing evidence for the strong sp^2 bonds throughout the structure. The D peak in the spectra is less evident, however still present in the 1360cm^{-1} region. A ratio between the D and G peaks was found to be 0.122, allowing the conclusion to be drawn that there are little defects in the graphene used, however, is not completely pristine, as there is a present D peak. Pristine, single-layered graphene also has an expected D2/G ratio of around 2, whereas the graphene used for this project shows a ratio of 0.542, showing the likelihood that it is multi-layered.

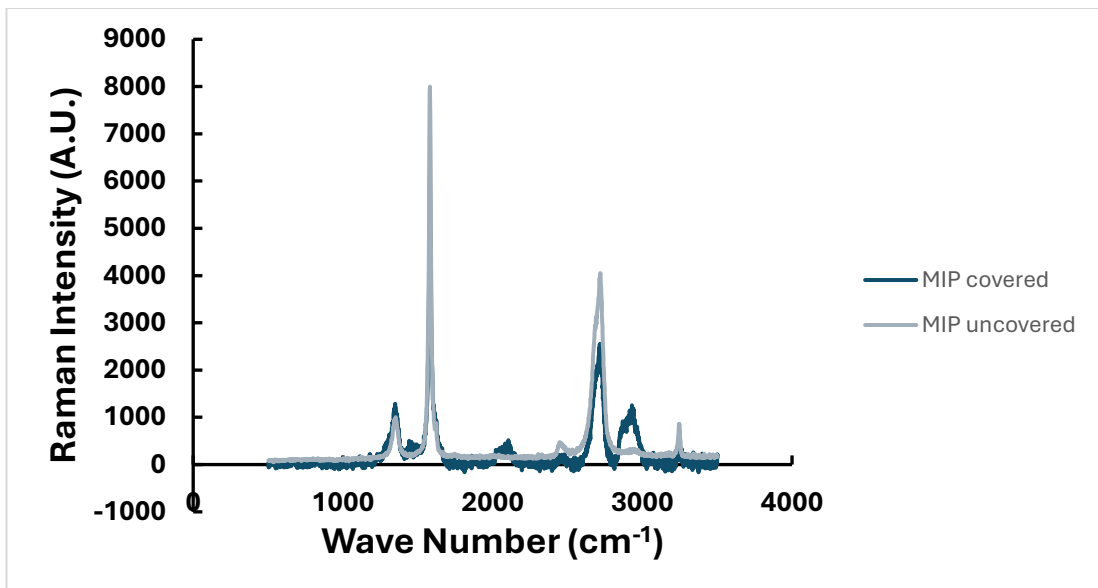


Figure 30: Raman spectroscopy data for both a molecularly imprinted polymer covered sensor (blue) and pre molecularly imprinted polymer application (grey)

During the project, Raman spectra for a sensor pre and post polymer application were obtained, showing similar results to the of the commercial graphene used, with peak intensities increasing, however ratios staying relatively similar. The D/G ratio of a covered sensor was found to be 0.229, while that of the uncovered sensor was 0.126. This shows the deviation in the ratio following polymer application, with figure 28 showing that the D peak is unchanged following application, however, the G peak intensity observes a relatively significant decrease. The primary difference in the spectra is the presence of a peak around 2940cm⁻¹, which is indicative of the polymer presence as a result of symmetric and asymmetric C-H stretching vibrations which are seen in these materials.

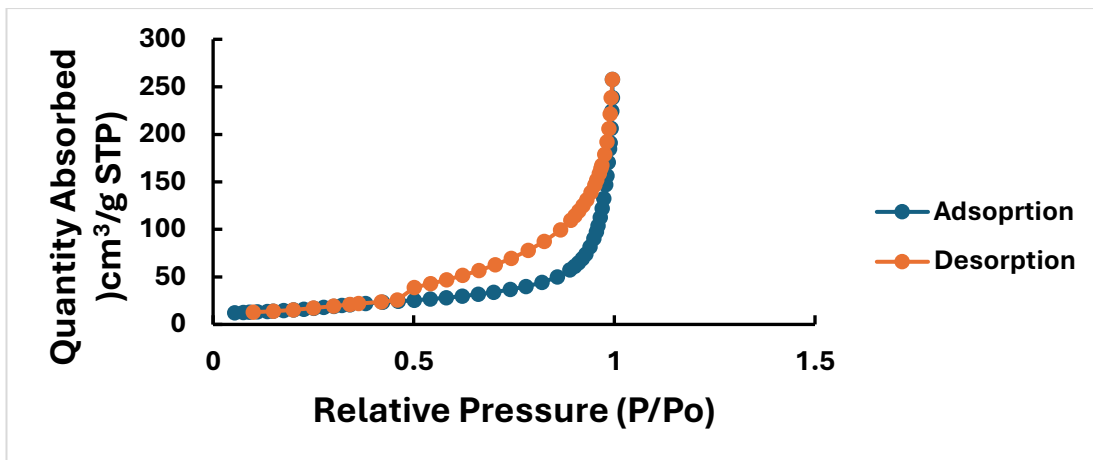


Figure 31: BET nitrogen adsorption analysis data for an uncovered sensor

BET nitrogen adsorption analysis data was taken for the carbon used throughout sensing, allowing for a type IV isotherm to be identified. This can allow for the identification of the carbon as mesoporous, displaying a steep initial rise at low relative pressures, indicating monolayer-multilayer adsorption on pore walls. The hysteresis loop present in the plot suggests capillary condensation in mesopores. Graphene-based carbons often contain mesopores forms by the assembly of graphene sheets, leading to a Type IV isotherm. Capillary condensation is also expected in a material of this form due to the pore size distribution in the mesoporous range of 2-50nm.

5.5 Electrochemical Sensing Performance

In order to assess the electrochemical performance of the sensor when used to determine concentration levels of MIB, a randle circuit with the Q element shown in figure 33 was chosen for all values such as the charge transfer resistance (R_{ct}) and the Warburg impedance (W). From here, a calibration curve was created from the R_{ct} value against the concentration of MIP in the testing solution. The decision to use the Q element was made due to the heterogeneous film coverage of the sensor surface while using the MIP, which can cause a deviation of the phase angle from the 90° which is expected from an ideal capacitor. From the use of both elements through testing, using the C element reduces the R^2 value further from 1, providing further reason for the choice.

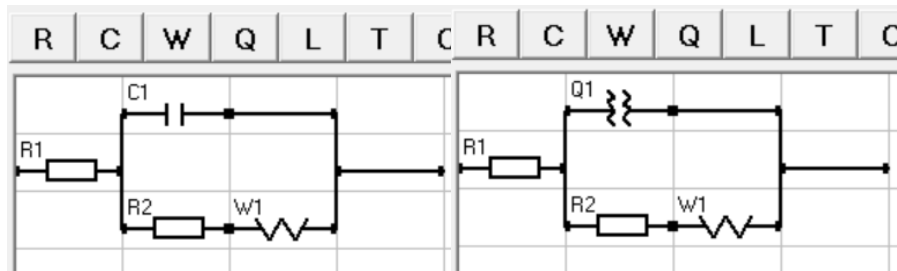


Figure 32: Randle circuit layout using both C and Q elements.

An ideal sensor was used to plot a calibration curve using the collected EIS data through concentrations of $10 - 100,000 \text{ ng/L}$ of MIB dissolved in deionised water. The calibration curve overall shows a linear trend with an ideal correlation between increasing R_{ct} response and an increasing MIB concentration, indicating successful binding interactions between the MIB molecules in the water and the binding sites present on the surface in concentrations as low as 10 ng/L . Each measurement was repeated to result in 3 values per concentration, allowing for error bars to be introduced based on the standard deviation of the repeats. Notably, as higher MIB concentrations the error bars become more pronounced, this suggests variability in sensor performance following increased concentration, potentially due to a saturation effect of binding sites on the surface resulting in more varied results.

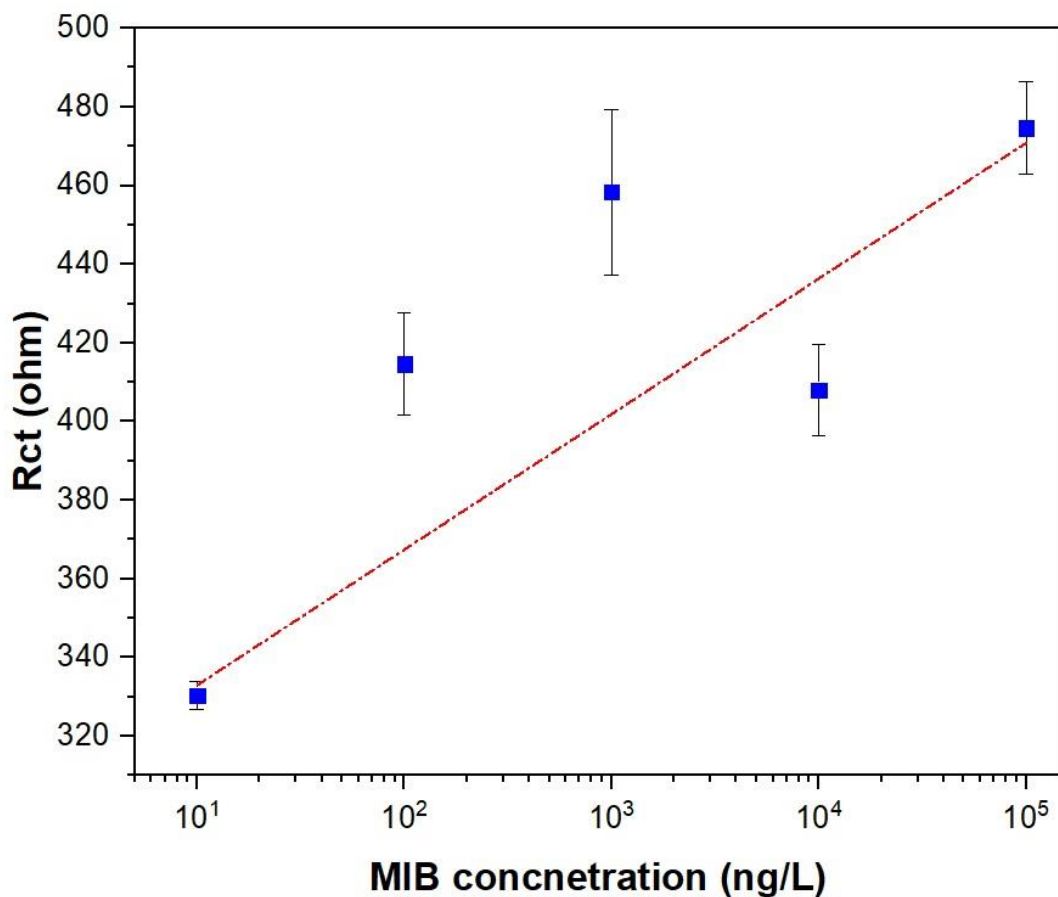


Figure 33: Calibration curve obtained for MIP using EIS data

The linear detection range of the sensor can be observed as the region where data points follow most accurately to the curve itself. In figure 30, the consistency of the range allows for the linear detection range to be identified as between 10ng/L and 100,000ng/L, however, further testing at a larger range of concentrations can be carried out to conclude whether it can be expanded outside of this. The R^2 value for the curve is 0.876, which indicated a relatively strong correlation between MIB concentration and the sensor's response within the range chosen. The sensitivity of the system was found through the change in R_{ct} per incremental increase in MIB concentration in the linear region, which was found using the first and final data point to be 0.00144 ohm/ng/L. Using the calibration curve data, the limit of detection was calculated to be 1.45ng/L, with the limit of quantification being calculated at 4.39 using the standard deviation of the intercept and the slope value of the curve, along with 3.3 and 10 for the limit of detection and quantification respectively.

5.6 Result Implication and Discussion

Initial results given for the comparison between base electrode materials was shown to be conclusive towards using the carbon-based electrode system, as these were produced in-lab, showed more consistent and ideal natured results, while having the prospect of using environmentally friendly materials for printing. Initial results also allowed for the conclusion of the drastic effect of the polymer application, with differing polymer volume, corresponding with a change in surface polymer layer thickness showing the desired results of a peak change decrease based on an increase in volume due to an increase in resistance.

Testing of surface area isolation methods were critical in the continuation of the research, allowing for the polymer so be isolated to the interdigitated section throughout the polymerization process. Epoxy was discovered to be the most efficient and consistent method of this in comparison to wax which was used initially. Issues presented with the use of wax is potentially as a result of prolonged exposure to higher than room temperature conditions, despite the melting temperature remaining above that used relatively significantly. Issues with this may also be as a result of the 48-hour polymerization time allowing for evaporation of polymer liquid or its constituents.

Thorough template removal solution testing allowed for the conclusion to use 1% ethanol alongside ultrasonication to encourage interaction between the ethanol present in the solution and the target molecules on the polymer surface. This decision was made due to the 100% ethanol, along with the methanol and acetic acid mixture having a drastic effect on both the NIP and MIP being tested on. This can be concluded to be caused by the erosive nature of the two solutions causing the removal of the surface of the polymer layer, causing recognition sites to be removed and the sensitivity of the sensor itself to be affected. The use of a 1% solution would allow for the erosive properties of ethanol to be minimized, while also being present to encourage the removal of template molecules, with EIS testing proving the ability for the template to be reintroduced post 1% ethanol removal, alongside minimal effect when tested with an NIP polymer layer.

The ability of the sensor to return to its initial electrochemical response following a 25-minute reintroduction period using a highly concentrated MIB solution allows for the conclusion to be drawn that in the time elapsed, all binding sites which were occupied post initial polymerisation are now reoccupied by the target molecule. This time is both ideal for testing repeatability, and allows for a baseline time frame to be used throughout testing as it indicates enough time passed to allow MIB molecules present in the solution to interact with the surface. Whether an increased time frame would be required incrementally as the concentration of solution decreased is unknown, however, 25-minutes was sufficient for final testing using as low as 10ng/L concentrations. For field sensor use, a minimal turn-around time for sensing and reintroduction would be ideal for repeated testing, with 25-minutes being satisfactory.

The sensitivity and limit of detection of the sensor is ideal, as despite the seemingly low sensitivity, environmental water concentration levels would allow for this to be ideal, alongside a limit of detection lower than that of the human nose or current detection techniques.

Chapter 6 Conclusion

The possibility of manufacturing an electrochemical biosensor for in-situ detection that is both sensitive and selective at incredibly low detection levels is shown to be entirely realistic, with a limit of detection of 1.45ng/L. The following conclusions can be drawn as a result of the research conducted:

- A graphene-based sensor is ideal in comparison to metal-based sensors due to the surface morphology allowing for better MIP interaction and cheaper production.
- A 48hour polymerization period is required for complete polymerization to occur using hexane as a solvent and MAA as the functional monomer for MIP synthesis for the chosen MIP volume.
- The ideal deposition volume for both electrochemical responses using CV testing and polymerization time was calculated to be 10mL.
- An oven curing time of 30 minutes was found to be optimal for the graphene-based sensor in comparison to 15 minutes.
- The desired template removal solution is 1% ethanol mixed with deionised water to avoid polymer destruction on the surface.
- A time frame of 25-minutes is ideal for both template removal and template reintroduction for time and binding site occupation efficiency.

The use of this sensor in the field would allow for the discontinuation of current detection techniques, allowing for less technical expertise to be required, less expensive equipment and fewer chemicals to be used in the process. The in-situ nature of the sensor would allow for significantly decreased turn around time for sensing results in comparison to that of current techniques and significantly decrease customer complaints due to MIB concentrations being detected at such trace levels.

For further expansion of this research project, electrochemical testing can be taken further for comparisons of sensitivity of the sensor to other, similarly structured compounds to ensure that field testing would not be affected by other contaminants, such as geosmin. A wider range of concentrations towards the limit of detection can be tested against the sensor, allowing for a more accurate limit to be calculated in a shorter linear range, allowing for repeatability of the sensors to be tested to ensure

that widespread manufacturing of sensors would be an industrial option. Further testing into the polymerization technique can be done to ensure the consistency of prepared sensors being eligible for testing.

The impact of MIPs on overall water detection has the potential to be taken into all impurity detection, allowing for incredibly sensitive detection, followed by removal of all water contaminants.

Bibliography

1. Neary et al., Linkages between forest soils and water quality and quantity. *Forest Ecology and Management*, 2009, 258(10), 2269- 2281.
2. Ying Ouyang, Evaluation of river water quality monitoring stations by principal component analysis. *Water Research*, 2005, 39(12), 2621-2635
3. Apramita Devi et al., Quantitative PCR based detection system for cyanobacterial geosmin/ 2-methylisoborneol (2-MIB) events in drinking water sources: Current status and challenges. *Water research*, 2021, 116478
4. H R Rogers, Factors causing off-taste in waters, and methods and practices for the removal of off-taste and its causes. Final Report to the Department of the Environment, Transport and the Regions, 2001.
5. P. Levallois and C.M. Villanueva, Drinking water quality and human health: an editorial. *International journal of environmental research and public health*, 2019, 16(4), 631.
6. N. Joseph, et al., A review of the assessment of sustainable water use at continental-to-global scale. *Sustainable Water Resources Management*, 2020, 6, 1-20.
7. S.G. Saad, Water and sanitation in hospitals integrated environmental management a serious forgotten issue. In Eleventh International Water Technology Conference, 2007, 695-701.
8. E.Ortenberg and B. Telsch, Taste and Odor Problems in portable Water. *Handbook of Water and Wastewater Microbiology Pages*, 2003, 777-793.
9. N.S.S. Anuar, et al., Characterization of Musty Odor-Producing Actinomycetes from Tropics and Effects of Temperature on the Production of Musty Odor Compounds. *Microbes and Environments*, 2017, 32(4), 352-357.
10. R. Srinivasan and G.A. Sorial, Treatment of taste and odor causing compounds 2-methyl isoborneol and geosmin in drinking water: A critical review. *Journal of Environmental Science*, 2011, 23(1), 1-13.
11. S.B. Watson, et al., Taste and odour and cyanobacterial toxins: impairment, prediction, and management in the Grate Lakes. *Canadian Journal of Fisheries and Aquatic Science*, 2008, 65(8), 1779-1796.

12. Saheed Mustapha, et al., A critical review on geosmin and 2-methylisoborneol in water: sources, effects, detection and removal techniques. 2021.
13. S.W. Krasner, et al., A standard method for quantification of earthy-musty odorants in water, sediments, and algal cultures. *Water Science and Technology*, 1983, 15(6-7), 127-138.
14. P.E. Persson, Off-flavours in aquatic ecosystems-an introduction. *Water Science and Technology*, 1983, 15(6-7), 1-11.
15. W.F. Young, et al., Taste and odour threshold concentrations of potential potable water contaminants. *Water Research*, 1996, 30(2), 331-340.
16. F. Juttner and S.B. Watson, Biochemical and Ecological Control of Geosmin and 2-Methylisoborneol in Source Waters. *Applied and Environmental Microbiology*, 2007, 73(14), 4395-4406.
17. World Health Organization, Guidelines for Drinking-Water Quality. Second Edition, Health Criteria and Other Supporting Information, 1996, 2, 64-65.
18. A. Mastropole, Evaluation of Available Scale-Up Approaches for the Design of GAC Contactors, 2011.
19. F. Edition, Guidelines for drinking-water quality. WHO chronicle, 2011, 38(4), 104-8.
20. C.J. Hwang, et al., Determination of Subnanogram-per-Liter Levels of Earthy-Musty Odorants in water by the Salted Closed-Loop Stripping Method. *Environmental Science Technology*, 1984, 18(7), 535-539.
21. W. Korth, et al., New standards for the determination of geosmin and methylisoborneol in water by gas chromatography/mass spectrometry. *Water Research*, 1991, 25(3), 319-324.
22. J-P.F.P. Palmentier, et al., The determination of geosmin and 2-methylisoborneol in water using isotope dilution high resolution mass spectrometry. *Water Research*, 1998, 32(2), 287-294.
23. A.J. Hassett, et al., Analysis of odorous compounds in water by isolation by closed-loop stripping with a multichannel silicone rubber trap followed by gas chromatography–mass spectrometry. *Journal of Chromatography A*, 1999, 849(2), 521-528.

24. J. Romero, et al., Validation of geosmin and 2-methyl-i-borneol analysis by CLSA-GC-FID method to obtain ISO-17025 accreditation. *Journal of Chromatography Science*, 2007, 45, 439-446.
25. A.K. Zander and P. Pingert, Membrane-based extraction for detection of tastes and odors in water. *Water Research*, 1997, 31(2), 301-309.
26. M.L. Bao, et al., Determination of trace levels of taste and odor compounds in water by microextraction and gas chromatography-ion-trap detection-mass spectrometry. *Water Research*, 1997, 31(7), 1719-1727.
27. J. Lu, et al., Trace analysis of off-flavor/odor compounds in water using liquid-liquid microextraction coupled with gas chromatography-positive chemical ionization-tandem mass spectrometry. *Frontiers of Environmental Science & Engineering*, 2016, 10(3), 477-481.
28. J. Lu, et al., Determination of earthy-musty odorous compounds in drinking water by vortex assisted dispersive liquid-liquid microextraction coupled with gas chromatography tandem mass spectrometry. *Analytical Sciences*, 2016, 32(4), 407-411.
29. R. McCallum, et al., Determination of geosmin and 2-methylisoborneol in water using solid-phase microextraction and gas chromatography-chemical ionization/electron impact ionization-ion-trap mass spectrometry. *Analyst*, 1998, 10, 2155-2160.
30. M.L. Bao, et al., Headspace solid-phase microextraction for the determination of trace levels of taste and odor compounds in water samples. *Analyst*, 1999, 124(4), 459-466.
31. S.B. Watson, et al., Quantitative analysis of trace levels of geosmin and MIB in source and drinking water using headspace SPME. *Water Research*, 2000, 34(10), 2818-2828.
32. S. Nakamura and S. Daishima, Simultaneous determination of 22 volatile organic compounds, methyl-tert-butyl ether, 1,4-dioxane, 2-methylisoborneol and geosmin in water by headspace solid-phase microextraction-gas chromatography-mass spectrometry. *Analytica Chimica Acta*, 2005, 548(1-2), 79-85.

33. Y.H. Sung, et al., Analysis of earthy and musty odors in water samples by solid-phase microextraction coupled with gas chromatography/ion trap mass spectrometry. *Talanta*, 2005, 65(2), 518-524.
34. K. Saito, et al., Determination of musty odorants, 2-methylisoborneol and geosmin, in environmental water by headspace solid-phase microextraction and gas chromatography-mass spectrometry. *Journal of Chromatography A*, 2008, 1186(1-2), 434-437.
35. J.F. Liu, et al., Development of polypropylene glycol coated hollow fiber membrane as passive sampler for field equilibrium sampling of odorous compounds in environmental waters. *Analytical Methods*, 2011, 3, 696-702.
36. M. Ligor and B. Buszewski, An Investigation of the Formation of Taste and Odour Contaminants in Surface Water Using the Headspace Spme-Gc/Ms Method. *Polish Journal of Environmental Studies*, 2006, 15(3), 429-435.
37. K. Ma, et al., Accurate analysis of trace earthy-musty odorants in water by headspace solid-phase microextraction gas chromatography-mass spectrometry. *Journal of Separation Science*, 2012, 35(12), 1494-1501.
38. X.C. Chen, et al., Simultaneous determination of ten taste and odor compounds in drinking water by solid-phase microextraction combined with gas chromatography-mass spectrometry. *Journal of Environmental Science*, 2013, 25(11), 2313-2323.
39. D.Y. Wu, et al., Quantitative analysis of earthy and musty odors in drinking water sources impacted by wastewater and algal derived contaminants. *Chemosphere*, 2013, 91(11), 1495-1501.
40. S.B. Yu, et al., Simultaneous determination of six earthy-musty odorous compounds in water by headspace solid-phase microextraction coupled with gas chromatography-mass spectrometry. *Analytical Methods*, 2014, 6(22), 9152-9159.
41. P. Zou, et al., Rapid and simultaneous determination of ten off-flavor compounds in water by headspace solid-phase microextraction and gas chromatography-mass spectrometry. *Journal of Central South University*, 2016, 23, 59-67.
42. K. Du, et al., Rapid Determination of Geosmin and 2-MIB in Water by Headspace Solid Phase Microextraction Gas Chromatography-Mass

Spectrometry. Proceedings -9th International Conference on Measuring Technology and Mechatronics Automation, ICMTMA, 2017, vol.2017.

- 43. M.L. Glykioti, et al., Room temperature determination of earthy-musty odor compounds in water using vacuum-assisted headspace solid-phase microextraction. *Analytical Methods*, 2016, 8(45), 8065-8071.
- 44. S.F. Peng, et al., Orthogonal Design Study on Factors Affecting the Determination of Common Odors in Water Samples by Headspace Solid-Phase Microextraction Coupled to GC/MS. *Journal of Analytical Methods in Chemistry*, 2013(1), 340658.
- 45. Z. Ding, et al., Analysis of Five Earthy-Musty Odorants in Environmental Water by HS-SPME/GC-MS. *International Journal of Analytical Chemistry*, 2014(1), 697260.
- 46. S.W. Lloyd, et al., Rapid analysis of geosmin and 2-methylisoborneol in water using solid phase microextraction procedures. *Water Research*, 1998, 32(7), 2140-2146.
- 47. J.P. Ma, et al., Determination of Geosmin and 2-Methylisoborneol in Water by Headspace Liquid-Phase Microextraction Coupled with Gas Chromatography-Mass Spectrometry. *Analytical Letters*, 2011, 44(8), 1544-1557.
- 48. Y. Ikai, et al., Determination of Geosmin and 2-Methylisoborneol in Water using Solid Phase Extraction and Headspace-GC/MS. *Journal of the Mass Spectrometry Society of Japan*, 2003, 51(1), 174-178.
- 49. W.F. Sun, et al., Simultaneous analysis of five taste and odor compounds in surface water using solid-phase extraction and gas chromatography-mass spectrometry. *Frontiers of Environmental Science & Engineering*, 2012, 6(1), 66-74.
- 50. E. Wright, et al., Development and validation of an SPE-GC-MS/MS taste and odour method for analysis in surface water. *International Journal of Environmental Analytical Chemistry*, 2014, 94(13), 1302-1316.
- 51. H. Kim, et al., Application of SPE followed by large-volume injection GC/MS for analysis of Geosmin and 2-Methylisoborneol in water. *Analytical Methods*, 2015, 7(16), 6678-6685.

52. Y. Huang, et al., Use of headspace solid-phase microextraction to characterize odour compounds in subsurface flow constructed wetland for wastewater treatment. *Waster Science and Technology*, 2004, 49(9), 89-98.
53. R.L. Bristow, et al., An extensive review of the extraction techniques and detection methods for the taste and odour compound geosmin (trans-1,10-dimethyl-trans-9-decalol) in water. *Trends in Analytical Chemistry*, 2019, 110, 233-248.
54. I.D. Wilson, et al., High-performance liquid chromatography-mass spectrometry (HPLC-MS)-based drug metabolite profiling. *Metabolic profiling: Methods and protocols*, 2011, 173-190.
55. K. Sato and S. Tanaka, Determination of Organic Compounds in water using the inhibitory effect of Luminol-Hydrogen Peroxide-Peroxodisulfate Chemiluminescence reaction. *Analytical Science*, 1991, 7(Supple), 1167-1170.
56. R. Sukor, Development of Immunoassays for the Detetion of 2-Methylisoborneol and Monensin in Water Samples. Doctoral dissertation, University of Guelph, 2013.
57. T.P. Hensarling and S.K. Waage, A bromine-based color reaction for the detection of geosmin. *Journal of Agricultural and Food Chemistry*, 1990, 38(5), 1236-1237.
58. S. Sand, et al., The current state of knowledge on the use of the benchmark dose concept in risk assessment. *Journal of Applied Toxicology: An International Journal*, 2008, 28(4), 405-421.
59. A. Alassi, et al., Quartz crystal microbalance electronic interfacing systems: A review. *Sensors*, 2017, 17(12), 2799.
60. H.S. Ji, et al., Increasing the sensitivity of piezoelectric odour sensors based on molecularly imprinted polymers. *Biosensors & Bioelectronics*, 2000, 15(7-8), 403-409.
61. G.S. Braga, et al., Molecularly imprinted polymer based sensor to detect isoborneol in aqueous samples. *Procedia engineering*, 2016, 168, 448-451.
62. J. Baranwal, et al., Electrochemical sensors and their applications: A review. *Chemosensors*, 2022, 10(9), 363.

63. J. Li, et al., Efficient electrochemical detection of geosmin in environmental waters. *Water Supply*, 2020, 20(6), 2206-2215.
64. T. Kamata, et al., Increased electrode activity during geosmin oxidation provided by Pt-nanoparticle-embedded nanocarbon film. *Nanoscale*, 2019, 11(18), 8845-8854.
65. Y. Wang et al., Electronic nose application for detecting different odorants in source water: Possibility and scenario. *Environmental Research*, 2023, 227, 115677.
66. C. Krantz-Rülcker, et al., Electronic tongues for environmental monitoring based on sensor arrays and pattern recognition: a review. *Analytica Chimica Acta*, 2001, 426(2), 217-226.
67. M. Son, et al., Real-time monitoring of geosmin and 2-methylisoborneol, representative odor compounds in water pollution using bioelectronic nose with human-like performance. *Biosensors and Bioelectronics*, 2015, 74, 199-206.
68. D.C. García, et al., Cross-linked poly (4-vinylphenol) in thin-film transistors for water analysis. In 2021 IEEE Latin America Electron Devices Conference (LAEDC) (pp. 1-4). IEEE.
69. G.S. Braga, et al., Performance of an electronic tongue during monitoring 2-methylisoborneol and geosmin in water samples. *Sensors and Actuators B: Chemical*, 2012, 171, 181-189.
70. F.L. Migliorini, et al., Tuning the electrical properties of electrospun nanofibers with hybrid nanomaterials for detecting isoborneol in water using an electronic tongue. *Surfaces*, 2019, 2(2), 432-443.
71. Anderson Lars, Sellergren Boerje, Mosbach Klaus, Imprinting of amino acid derivatives in macroporous polymers. *Tetrahedron Letters*. 1984, 25, 5211-5214.
72. Wulff. G, Sarhan. A, Zabrocki. K. Enzyme- analog built polymers and their use for resolution of racemates. *Tetrahedron Letters*. 1973, 14, 4329-4332.
73. Toshifumi Takeuchi et al., Signalling molecularly imprinted polymers: molecular recognition-based sensing materials. *The chemical record*. 2005, 5(5), 263-275.

74. Joseph J. BelBruno, Molecularly Imprinted Polymers. *Chemical Reviews*. 2019, 119, 94-119.

75. Björn C. G. Karlsson et al., Structure and Dynamics of Monomer- Template Complexation: An Explanation for Molecularly Imprinted Polymer Recognition Site Heterogeneity. *Journal of the American Chemical Society*. 2009, 131, 13297-13304.

76. Romana Schirhagl, Bioapplications for Molecularly Imprinted Polymers. *Analytical Chemistry*. 2014, 86, 250-261.

77. Jun Matsui et al., Molecular Recognition in Continuous Polymer Rods Prepared by a Molecular Imprinting Technique. *Analytical Chemistry*. 1993, 65, 2223-2224.

78. Jun Matsui et al., Rod-Type Affinity Media for Liquid Chromatography Prepared by in-situ-Molecular Imprinting. *Analytical Sciences*. 1995, 2, 1017-1019.

79. Oliver Brüggemann et al., New configurations and applications of molecularly imprinted polymers. *Journal of Chromatography A*. 2000, 889(1-2), 15-24.

80. Andersson L.I. et al., A highly selective solid phase extraction sorbent for preconcentration of sameridine made by molecular imprinting. *Chromatographia*. 1997, 46(1-2), 57-62.

81. Georgios Theodoridis et al., Automated sample preparation based on the sequential injection principle: Solid phase extraction on a molecularly imprinted polymer coupled on-line to high-performance liquid chromatography. *Journal of Chromatography A*. 2004, 1030(1-2), 69-76.

82. Börje Sellergren, Direct Drug Determination by Selective Sample Enrichment on an Imprinted Polymer. *Analytical Chemistry*. 1994, 66, 1578-1582.

83. Wayne M. Mullet and Edward P.C. Lai, Determination of Theophylline in Serum by Molecularly Imprinted Solid-Phase Extraction Pulsed Elution. *Analytical Chemistry*. 1998, 70(17), 3636-3641.

84. Wayne M. Mullett et al., Multidimensional on-line sample preparation of verapamil and its metabolites by a molecularly imprinted polymer coupled to liquid chromatography-mass spectrometry. *Journal of Chromatography B*. 2004, 801(2), 297-306.

85. P.D. Martin et al., Comparison of extraction of a β -blocker from plasma onto a molecularly imprinted polymer with liquid-liquid extraction and solid phase extraction methods. *Journal of Pharmaceutical and Biomedical Analysis*. 2004, 35(5), 1231-1239.

86. Ester Caro et al., A new molecularly imprinted polymer for the selective extraction of naproxen from urine samples by solid-phase extraction. *Journal of Chromatography B*. 2004, 813(1-2), 137-143.

87. Ester Caro et al., Direct determination of ciprofloxacin by mass spectrometry after a two-step solid-phase extraction using a molecularly imprinter polymer. *Journal of Separation Science*. 2006, 29(9), 1230-1236.

88. Jianchun Xie et al., Selective extraction of functional components derived from herb in plasma by using a molecularly imprinted polymer based on 2,2-bis(hydroxymethyl)butanol trimethacrylate. *Journal of Chromatography B*. 2003, 788(2), 233-242.

89. Mark T. Muldoon and Larry H. Stanker, Molecularly Imprinted Solid Phase Extraction of Atrazine from Beef Liver Extracts. *Analytical Chemistry*. 1997, 69, 803-808.

90. Edward P.C. Lai and Stanley G. Wu, Molecularly imprinted solid phase extraction for rapid screening of cephalexin in human plasma and serum. *Analytical Chimica Acta*. 2003, 481(2), 165-174.

91. Cobb Zoe et al., Water-compatible molecularly imprinted polymers for efficient direct injection on-line solid-phase extraction of ropivacaine and bupivacaine from human plasma. *Analyst*. 2007, 132(12), 1262-1271.

92. Marinah M. Ariffin et al., Molecularly Imprinted Solid-Phase Extraction of Diazepam and Its Metabolites from Hair Samples. *Analytical Chemistry*. 2007, 79, 256-262.

93. Hongyuan Yan and Kyung Ho Row, Novel molecularly imprinted monolithic column for selective on-line extraction of ciprofloxacin from human urine. *Biomedical Chromatography*. 2008, 22(5), 487-493.

94. F. Hugon-Chapuis et al., Selective and automated sample pretreatment by molecularly imprinted polymer for the analysis of the basic drug alfuzosin from plasma. *Journal of Chromatography A*. 2008, 1196-1197, 73-80.

95. Antoni Beltran et al., Selective solid-phase extraction of amoxicillin and cephalaxin from urine samples using a molecularly imprinted polymer. *Journal of Separation Science*. 2008, 31(15), 2868-2874.
96. A. Beltran et al., Synthesis by precipitation polymerisation of molecularly imprinted polymer microspheres for the selective extraction of carbamazepine and oxcarbazepine from human urine. *Journal of Chromatography A*. 2009, 1216(12), 2248-2253.
97. S. Vo Duy et al., Molecularly imprinted polymer for analysis of zidovudine and stavudine in human serum by liquid chromatography-mass spectrometry. *Journal of Chromatography B*. 2009, 877(11-12), 1101-1108.
98. M. T. Jafari et al., Ion Mobility Spectrometry as a Detector for Molecular Imprinted Polymer Separation and Metronidazole Determination in Pharmaceutical and Human Serum Samples. *Analytical Chemistry*. 2009, 81, 3585-3591.
99. Martina Lasáková et al., Molecularly imprinted polymer for solid-phase extraction of ephedrine and analogues from human plasma. *Journal of Separation Science*. 2009, 32(7), 1036-1042.
100. C. Ferrag and K. Kerman, Grand challenges in nanomaterial-based electrochemical sensors. *Frontiers in Sensors*, 2020, 1, 583822.
101. J.F. Hernández-Rodríguez, et al., Electrochemical sensing directions for next-generation healthcare: trends, challenges, and frontiers. *Analytical Chemistry*, 2020, 93(1), 167-183.
102. Khalid, M. A. A, *Redox Principles and Advanced Applications*. 2017.
103. Joseph Wang, *Analytical Electrochemistry*, Third Edition, Fundamental Concepts. 2006.
104. Allen J. Bard and Larry R. Faulkner, *Electrochemical Methods: Fundamentals and Applications* Second Edition. 2001.
105. Bansi D. Malhorta, et al., Prospects of conducting polymers in biosensors. *Analytica Chimica Acta*. 2006, 578(1), 59-74.
106. Azad Mohammad and Avin Abdullah, *Scanning Electron Microscopy: A Review*. *Proceedings of 2018 International Conference on Hydraulics and Pneumatics – HERVEX*. 2018, 77-85.

107. Gurvinder S. Bumbrah and Rakesh M. Sharma, Raman spectroscopy – Basic principle, instrumentation and selected applications for the characterization of drugs and abuse. Egyptian Journal of Forensic Sciences. 2016, 6(3), 209-215

108. Stephen Brunauer, P. H. Emmett and Edward Teller, Adsorption of Gases in Multimolecular Layers. Contribution from the Bureau of Chemistry and Soils and George Washington University. 1938, 309-319.

109. Giuseppe Vasapollo et al, Molecularly Imprinted Polymers: Present and Future Prospective. 2011, 12(9), 5908- 5945.

Appendices: Materials and Methodology

Figure 34: FlexiProof Rolling press printer used for sensor production



Figure 35: Oven used for sensor optimisation



Figure 36: Finalisation of printing process on polyimide sheet